



UNIVERSITI PUTRA MALAYSIA

***AN EVALUATION OF AN EXOSKELETON TO ASSIST POLE HANDLING
DURING MANUAL OIL PALM HARVESTING ACTIVITY***

MUHAMMAD AIZAT BIN AB AZIZ

**Ip
FK 2019 69**

**AN EVALUATION OF AN EXOSKELETON TO ASSIST POLE HANDLING
DURING MANUAL OIL PALM HARVESTING ACTIVITY**

MUHAMMAD AIZAT BIN AB AZIZ

184390

**BACHELOR OF ENGINEERING
(AGRICULTURAL & BIOSYSTEM)**

**FACULTY OF ENGINEERING
UNIVERSITI PUTRA MALAYSIA**

2018/2019

I. Approval Sheet

This project report here to entitle “AN EVALUATION OF AN EXOSKELETON TO ASSIST POLE HANDLING DURING MANUAL OIL PALM HARVESTING ACTIVITY” was prepared and submitted by MUHAMMAD AIZAT BIN AB AZIZ in partial fulfilment of the requirement for the degree of Bachelor of Engineering (Agricultural and Biosystem) is hereby accepted.

Approved by:

.....

(Dr. Hazreen Haizi bt. Harith)

Project Supervisor

Date:

Approved by:

.....

(Dr. Mahirah bt. Jahari)

Project Examiner

Date:

Approved by:

.....

(Dr. Sharence Nai Sowat)

Project Examiner

Date:

II. Acknowledgement

In the name of Allah, The Most Gracious, The Most Merciful.

My thanks and appreciations goes every person in developing the project and people who have willingly helped me out with their abilities. It would not have been possible without the kind support and help of many individuals.

First and foremost, my deep appreciation and gratitude goes to my supervisor, Dr. Hazreen Haizi bt. Harith, who expertly guided me through her advice, guidance and encouragement without which this project would not have been possible. Her unwavering support kept me constantly focused with my work and engaged on what I had done.

My sincere appreciation and thanks also towards my examiners, Dr. Mahirah bt. Jahari and Dr. Sharence Nai Sowat who helped me directly or indirectly in completing my experiment. Also, many thanks to my colleagues for their willingness to help and guide me throughout the completion of the project.

I would like express my gratitude towards my parents, late Ab. Aziz bin Mat Sanishah and Fadzilah binti Ab. Rahman , and all my family members for their kind co-operation and encouragement which help me in completion of this project.

III. Table of Content

I.	Approval Sheet.....	2
II.	Acknowledgement.....	3
III.	Table of Content.....	4
IV.	Abstract.....	6
V.	Abstrak.....	7
VI.	List of Figures.....	8
Chapter 1:	Introduction.....	11
1.1	General Overview.....	11
1.1.1	Harvesting Tools and Practices.....	11
1.1.2	Advantages of upper limb Exoskeleton.....	13
1.1.3	Importance of Motion Study for manual harvesting activities.....	15
1.2	Problem Statement.....	16
1.3	Objectives.....	16
Chapter 2:	Literature Review.....	16
2.1	IMU Sensors and the Components.....	17
2.2	Previous Researches Using IMU Sensors.....	19
2.3	IMU Sensor Calibration.....	20
2.4	Fusion Filters.....	21
2.5	Conclusion.....	22

Chapter 3: Methods.....	23
3.1 General Overview	23
3.2 Experimental Procedure	25
Chapter 4: Results and Discussion.....	29
4.1 IMU Sensor Calibration and Orientation	29
4.2 Impact of the Exoskeleton toward motion of limbs	31
Chapter 5: Conclusion and Recommendation.....	58
5.1 Conclusion.....	58
5.2 Recommendation.....	59
5.2.1 Recommended workflow	59
5.2.2 Future of this project.....	59
References.....	60
Appendix.....	63
Standard Operating Procedure	63
Hardware	63
Setting Up Hardware Connection.....	64
Inertia Motion Unit (Mtw) Placement	65
Monitoring Mtw	67
Additional Information	68

IV. Abstract

The integration between robots and humans offers new opportunities for the creation of new assistive technologies that can be used in the field of agriculture. However, research analysing the impact of using exoskeleton on users' limbs movement is limited. In this paper, we used IMU sensors to capture human motion data. Based on the motion data, the graphs of angle of motion against time were plotted. Thus, we can understand the impact of exoskeleton in assisting pole handling during manual harvesting. The motion data includes how the limbs of the subjects move, degree of angle of the subjects' limbs. Analysis of the motion data showed that wearing exoskeleton causes lower motion angle. Note that the amplitude given by the IMU sensors correspond to the limb angle. When the amplitude of motion angle is lower, the limbs movements are also less compared to limbs movement when not wearing exoskeleton, which suggests reduced muscle activity when wearing exoskeleton. Perhaps by wearing an exoskeleton, the workers may consume less energy as there is support from exoskeleton to support the load.

V. Abstrak

Integrasi antara robot dan manusia menawarkan peluang baru untuk mewujudkan teknologi bantuan baru yang boleh digunakan dalam bidang pertanian. Walau bagaimanapun, penyelidikan menganalisis impak menggunakan exoskeleton pada pergerakan anggota pengguna adalah terhad. Dalam hal ini, kami menggunakan sensor IMU untuk merekod data gerakan manusia. Berdasarkan data gerakan, graf sudut gerakan terhadap masa telah diplotkan. Oleh itu, kita dapat memahami kesan exoskeleton dalam membantu pengendalian tiang semasa penuaian manual. Data pergerakan termasuk bagaimana pergerakan subjek bergerak, tahap sudut anggota subjek. Analisis data gerakan menunjukkan bahawa memakai exoskeleton menyebabkan sudut pergerakan yang lebih rendah. Perhatikan bahawa amplitud yang diberikan oleh sensor IMU sesuai dengan sudut anggota badan. Apabila amplitud sudut gerakan lebih rendah, pergerakan anggota badan juga kurang berbanding pergerakan anggota badan apabila tidak memakai exoskeleton, yang menunjukkan aktiviti otot berkurang apabila memakai exoskeleton. Mungkin dengan memakai exoskeleton, pekerja mungkin menggunakan tenaga kurang kerana ada sokongan dari exoskeleton untuk menyokong beban.

VI. List of Figures

Figure 1.1: Elements of work process harvesting palm plantation.....	11
Figure 1.2: A worker carry harvest pole	13
Figure 1.3: A worker raising a tall harvesting pole to cut palm fruit from high in the trees... ..	13
Figure 1.4: A worker cutting frond and fruits bunches.....	13
Figure 1.5: A worker collecting fresh fruit bunch (FFB).....	13
Figure 1.6: Example of upper limb exoskeleton.....	15
Figure 2.1: Euler angles orientation representation.	17
Figure 2.2: Simplified explanation of accelerometer, gyroscope and magnetometer.....	19
Figure 2.3: T-pose for sensor calibration	21
Figure 3.1: Summary of motion data acquisition in flowchart	24
Figure 3.2: Subject 1 without exoskeleton.....	26
Figure 3.3: Subject 1 wearing exoskeleton	26
Figure 3.4: Subject 2 without exoskeleton.....	26
Figure 3.5: Subject 2 wearing exoskeleton	26
Figure 3.6: Subject 3 without exoskeleton.....	26
Figure 3.7: Subject 3 wearing exoskeleton	26
Figure 3.8: Activity 1 (Calibration of sensors)	27
Figure 3.9: Activity 2 (Lift up pole)	27
Figure 3.10: Activity 3 (Tugging).....	27
Figure 3.11: Activity 4 (Lift down pole)	27
Figure 3.12: Activity 5 (Recalibration).....	27
Figure 3.13: Illustration of IMU sensors location at subject's limbs	28
Figure 4.1: Orientation of sensor when motion data is near to $(0^\circ, 0^\circ, 0^\circ)$	29
Figure 4.2: IMU sensor orientation when roll motion data is positive	31

Figure 4.3: IMU sensor orientation when roll motion data is negative	31
Figure 4.4: IMU sensor orientation when pitch motion data is positive.....	31
Figure 4.5: IMU sensor orientation when pitch motion data is negative.....	31
Figure 4.6: IMU sensor orientation when yaw motion data is positive	31
Figure 4.7: IMU sensor orientation when yaw motion data is negative	31
Figure 4.8: Graphs for roll motion data at coccyx. (a) Subject number 1. (b) Subject number 2. (c) Subject number 3.....	32
Figure 4.9: Location of an IMU sensor at coccyx	33
Figure 4.10: Graphs for pitch motion data at coccyx. (a) Subject number 1. (b) Subject number 2. (c) Subject number 3.....	34
Figure 4.11: Graphs for roll motion data at right scapula. (a) Subject number 1. (b) Subject number 2. (c) Subject number 3.....	36
Figure 4.12: Graphs for roll motion data at left scapula. (a) Subject number 1. (b) Subject number 2. (c) Subject number 3.....	37
Figure 4.13: IMU sensors location at left scapula and right scapula	38
Figure 4.14: Graphs for pitch motion data at right scapula. (a) Subject number 1. (b) Subject number 2. (c) Subject number 3.....	39
Figure 4.15: Graphs for pitch motion data at left scapula. (a) Subject number 1. (b) Subject number 2. (c) Subject number 3.....	40
Figure 4.16: Graphs for yaw motion data at right scapula. (a) Subject number 1. (b) Subject number 2. (c) Subject number 3.....	42
Figure 4.17: Graphs for yaw motion data at left scapula. (a) Subject number 1. (b) Subject number 2. (c) Subject number 3.....	43
Figure 4.18: Graphs for roll motion data at right humerus. (a) Subject number 1. (b) Subject number 2. (c) Subject number 3.....	45

Figure 4.19: IMU sensors location at humerus, radius and metacarpal.....	46
Figure 4.20: Graphs for pitch motion data at right humerus. (a) Subject number 1. (b) Subject number 2. (c) Subject number 3.....	47
Figure 4.21: Graphs for roll motion data at left humerus. (a) Subject number 1. (b) Subject number 2. (c) Subject number 3.....	49
Figure 4.22: Angular movement: abduction, adduction, and circumduction of the upper limb	51
Figure 4.23: Graphs for pitch motion data at right radius. (a) Subject number 1. (b) Subject number 2. (c) Subject number 3.....	52
Figure 4.24: Graphs for pitch motion data at left radius. (a) Subject number 1. (b) Subject number 2. (c) Subject number 3.....	53
Figure 4.25: Adduction when wearing exoskeleton	54
Figure 4.26: Adduction when not wearing exoskeleton	54
Figure 4.27: Graphs for yaw motion data at right radius. (a) Subject number 1. (b) Subject number 2. (c) Subject number 3.....	55
Figure 4.28: Graphs for yaw motion data at left radius. (a) Subject number 1. (b) Subject number 2. (c) Subject number 3.....	56

Chapter 1: Introduction

1.1 General Overview

1.1.1 Harvesting tools and practices

In manual harvesting process, there are three common tools which are a chisel that is attached to a short steel pole, and it is used to harvest young palms that are about 3 metres high. For harvesting taller trees (taller than 3 metres), the workers use a pruning hook or sickle attached to a long pole. But when the trees reached the height of 15 metres, an extensible poles will be use to harvest fruit bunches (Abdul Razak Jelani et al., 2008).

Conventionally, the harvesting task of palm use Aluminium Pole Knife (APK) (Saibani et al., 2015). While the working process of harvesting is demonstrated in Figure 1.1.

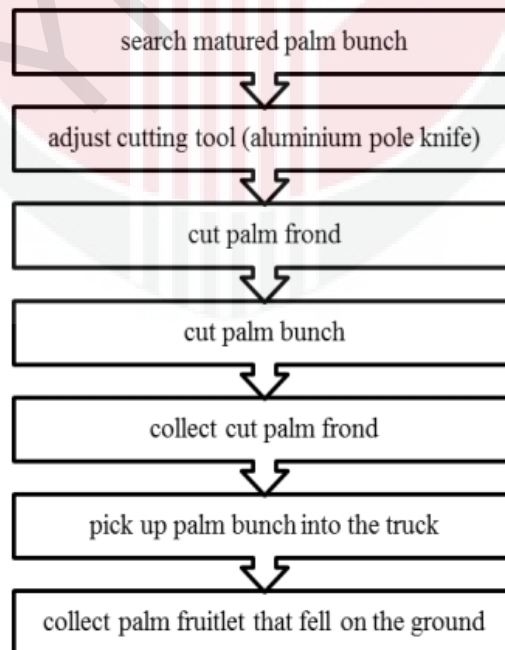


Figure 1.1: Elements of work process harvesting palm plantation.

Technics in handling tools are important in the harvesting process. To ensure efficient cutting, the harvesting tools are targeted at the target point (frond base or bunch stalk) at a very high rate. In combination with the weight of the instruments and high cutting speed produces high momentum which gives sufficient energy to cut through the fronds (Abdul Razak Jelani et al., 2008).

Other activities in harvesting that the workers must carry out besides cutting FFB are lifting the pole and carrying the pole upright. Depending on oil palm tree age and planting material, each palm may yield between 8 as well as 15 FFB annually and weighing between 15 and 25 kg each (Abdul Razak Jelani et al., 2008). After cutting activity, lifting and carrying pole are also exhausting and energy consuming. Another factor that making harvesting activities consume high energy is because of the tools' weight which can reached 8 kilograms.

From Figure 1.2 to Figure 1.5 show harvesting activities in oil palm plantation by the workers. In Figure 1.2: A worker carry harvest pole. Before harvesting, the worker need to raise a tall harvesting pole to cut palm fruit from high in the trees as shown in Figure 1.3. Only then, the worker proceed to cutting frond and fruits bunches as in Figure 1.4. In Figure 1.5 as the final step in harvesting activities.



Figure 1.2: A worker carry harvest pole



Figure 1.3: A worker raising a tall harvesting pole to cut palm fruit from high in the trees.



Figure 1.4: A worker cutting frond and fruits bunches



Figure 1.5: A worker collecting fresh fruit bunch (FFB)

1.1.2 Advantages of upper limb exoskeleton

The plantation labour workers are prone to muscle strain when performing harvesting activities. Muscle strain is a condition where tearing occurs due to the sudden extension of a joint beyond its normal range of function or by any other excessive physical demand made on the muscle (Ma and Ma, 2011). This type of injury to the biceps brachii or the pectoralis major and pectoralis minor can occur while the worker undergoes tugging activity or collecting fresh fruit bunch (FFB). The workers may feel stiffness, tenderness, or pain in the affected muscles, and motion in the affected joints may be limited (Ma and Ma, 2011).

To prevent this particular problem, implementation of the exoskeletons in the plantation is particularly beneficial. Exoskeletons are wearable devices that work in tandem with the user (Gonzalez, 2017). In addition to that, exoskeleton is placed on the user's body and act as amplifiers that augment, reinforce or restore human performance. Exoskeletons can cover the entire body, just the upper or lower extremities, or even a specific body segment such as the ankle or the hip. In this study, we focused only on upper extremities exoskeleton.

Exoskeleton is used to support the arms of professionals and skilled workers who carry out recurrent arm movements and/or fixed arm raising (work at or above the head) (Modic, 2018). With the aid from exoskeleton, the weight of the user's arms is transferred back and forth to the core (Modic, 2018). Similarly, exoskeleton also gives three main advantages to the wearer, which are significant decrease of injury issues at the workplace, reduced medical costs and reduced sick leave (Gonzalez, 2017; Modic, 2018).

Other than that, exoskeleton also should lower workers' exhaustion which may result in increased alertness, productivity and quality of work (Gonzalez, 2017; Yagi et al., 2016). Also, upper limb exoskeleton lifts as well as upholds the labourers' arm in activities from chest to overhead. The profile is small and easy to wear, allowing freedom of movement, in all conditions (Akdoğan, 2019; Gonzalez, 2017; Modic, 2018).



Figure 1.6: Example of upper limb exoskeleton.

Another main goal of the development an exoskeleton was to assist the worker to support the load rather than solely let the muscle support the weight. The support in exoskeleton will aiding the workers' elbows and shoulders in lifting and preventing the load strained the labours excessively (Yagi et al., 2016).

A new finding shows that exoskeleton are relevant in Malaysia because implementation of exoskeleton in the plantation will help boosting productivity of the labours (Gonzalez, 2017; Namikawa, 2012) and to keep up with aging and to cope with difficulty in harvesting activities (Toyama and Yamamoto, 2009). The implementation of exoskeleton helps in harvesting and pruning thus aimed at making it industry and task-specific.

1.1.3 Importance of motion study for manual harvesting activities

In the oil palm industry, time and motion studies have now been widely accepted for evaluation of harvesting tasks (Saibani et al., 2015). A great number of time and motion study results are being used to improve work efficiency in the sector.

By study motion and time, we can identify and measure the efficiency of the manual oil palm fruit bunches harvesting technique (Saibani et al., 2015). Time and motion study is a

means to justification for the need of mechanical system to accelerate the process of harvesting palm fruit and increase the productivity.

Time and motion study's aim is to get rid of unnecessary work with an addition to provide measurements for determining the performance of harvesting tasks. The study helps to examine the effective and non-effective motions used by the harvester in the harvesting process (Saibani et al., 2015).

1.2 Problem Statement

When the plantation workers undergoes manual harvesting without any external support, they are exposed to musculoskeletal injuries because of the weight load from tools or fresh fruit bunch (FFB) (Abdul Razak Jelani et al., 2008). Other than that, the workers' health also may be effected by their bad body posture when carrying harvesting tools. They are also prone to muscle soreness when lifting load without external support or when doing repetitive activities.

The purposes of this experiment is to evaluate how exoskeletons as wearable devices can assist the workers when handling harvesting tools. Besides that, we want to assess the effects of wearing exoskeleton towards the movement of limbs.

1.3 Objectives

- I. To assess the impact of using exoskeleton for pole handling during manual harvesting.
- II. To configure the MTw Awinda system manufactured by Xsens (Enschede, the Netherlands) for collecting motion data in laboratory and outdoor operation.

Chapter 2: Literature Review

2.1 IMU Sensors and the Components

The IMU is a 3-axis electronic device designed to estimate the orientation of the sensor and its motion (Matula, 2016). Also, IMU is used primarily in velocity, orientation and gravitational strength measurement devices. These miniature sensors include an embedded processor to calculate absolute orientation (roll, pitch, and yaw), acceleration, angular velocity and North directional in real time (Pérez et al., 2010).

The IMU sensor technology consists of 3D gyroscope, 3D accelerometer and 3D magnetometer in one package (Ahmad et al., 2014; Paulich et al., 2018; Saibani et al., 2015). IMU usually takes measures in three axes, totalling nine DOF, in three different axes (Ahmad et al., 2014). Inertial Measurement units (IMUs), in order to accurately estimate the orientation of a fixed framework, are based on the use and combination of various inertial sensors technologies such as accelerometers, gyroscopes and magnetometers (Pérez et al., 2010).

According to Matula (2016), The IMU has been measuring its orientation towards to the fixed frame on earth. The data can be displayed in various forms, but the Euler (pitch, roll, and yaw) is the most dominant. Figure 2.1 shows Euler angles orientation representation from IMU sensors.

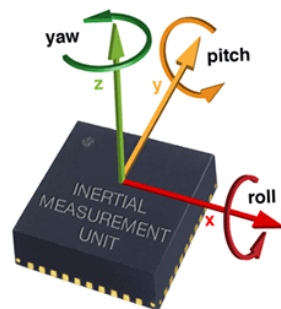


Figure 2.1: Euler angles orientation representation.

The accelerometer has been used to make measurements of inertial acceleration (Ahmad et al., 2014). While Matula (2016) define accelerometers as electromechanical devices which measure the acceleration rate, typically in meters per second squared. Furthermore, an accelerometer certainly senses static forces like gravity and dynamic forces like motion or vibration (Matula, 2016). The accelerometer is based on Newton's second law of motion, the calculation force F , with a constant scaling meter called a proof mass (Kajánek, 2008).

$$F = m \cdot a$$

Gyroscope is an inertial sensing system used to measure the body's rotational rate (measured in degrees / s) (Ahmad et al., 2014). Matula (2016) expressed that the digital gyroscope known as the angular velocity sensor and a sensing instrument that rotates an axis, usually in degrees per second angle velocity. Pérez et al. (2010) added; gyroscopes measure the angular velocity applied to the object and thus the rotated angle and current orientation, where there is an initial reference. In addition, Paulich et al. (2018) said that when gyroscope data integrated over time, it provides an estimate of the change in orientation.

Jain (2008) explained the use of a magnetometer to measure the direction and strength of the magnetic field. Paulich et al. (2018) says the same statement by stating a 3D magnetometer is able to measure strength and direction of the surrounding magnetic field. Ahmad et al. (2014) added magnetometer attempts to measure the magnetic particular direction of the bearing and therefore can improve gyroscope reading.

In addition, Matula (2016) stated that the Earth's magnetic field can be used as a compass, if it's the only magnetic field acting on a sensor to determine the direction of the sensor to the Earth North Pole. Paulich et al. (2018) also said that the magnetometer measures the Earth magnetic field if no magnetic disturbances are present.

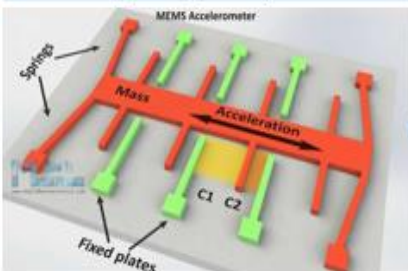
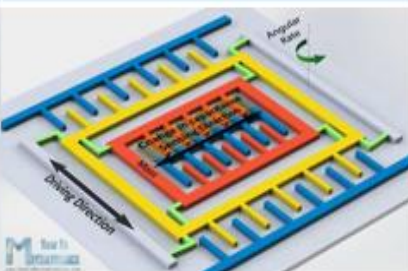
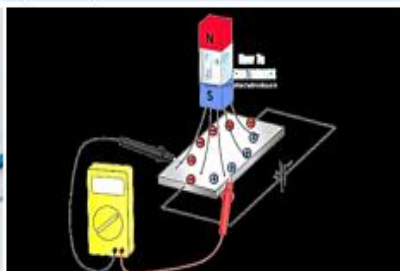
Accelerometer	Gyroscope	Magnetometer
measures acceleration by measuring change in capacitance	measures angular rate using the Coriolis Effect	measures the earth magnetic field by using Hall Effect
		

Figure 2.2: Simplified explanation of accelerometer, gyroscope and magnetometer.

2.2 Previous Researches Using IMU Sensors

Pérez et al. (2010) have developed a sensor-based inertial monitoring system is presented to measure and analyse the movements of the top limbs. The researched is about portable upper limb motion analysis system for neuro-rehabilitation based on inertial technology. The main objective of the current study was the development of a real-time portable upper limb motion acquisition system for the upper limb and the preliminary validation of a therapeutic evaluation that would be accurate.

O'Donovan et al. (2007) describes the design and evaluation of the three-dimensional (3D) joint angle measuring technique for the miniature kinematic sensor. The technology makes 3D intersegment joint angle measurement possible and can be beneficial in a number of applications requiring joint angles monitoring. The technique does not depend on a fixed coordinate system for references, so it can be used in a dynamic system. The procedure was assessed through applying it to ankle joint angle measurement. Experimental results show that the technique is used to accurately measure the ankle joint angles.

Hirose et al. (2013) proposes the method of dynamic movement analysis for ski turns with inertial and strength sensors. By informing inertial sensors using Unscented Kalman

filters, this method can estimate the Roll-Pitch-Yaw angle in local coordinates. The results of the analysis with a joint torque show the gliding forces of the skiers on the actual snowfield. The method of analysis and results can therefore be applied to evaluate the ability of turns and resolve the ski turning mechanism.

Cavallo et al. (2014) undergoes research focuses on the development and implementation of the attitude and heading reference system (AHRS), highly precise device systems and fast sensor data fusion algorithms to approximate the orientation of a rigid body towards the reference framework. More specifically, the gradient-based descent algorithm and the non-linear complementary filter-based algorithm are compared with standard Extended Kalman Filter (EKF). This is to demonstrate that an overall method can easily compete with and even overcome ad-hoc solutions under specific conditions.

Seel et al. (2014) contribution which is related to joint angle calculation based on human motion analysis inertial measurement data. Concentrate on methods to avoid assuming certain orientations in respect of body segments in which the sensors are fitted. Provide results from transfemoral amputee gait studies in which an optical 3D move-capture system compares inertial unit (IMU)-based methods.

2.3 IMU Sensor Calibration

Sensors calibration are done by following simple quaternion-based estimation methods by YEI Technology (Labs, 2013). They propose that quaternions are used for the sensors to compute downward with forward vectors and requires an initial calibration by standard T-position. T-pose for calibration is when arms directly off the body's side and palms forward as shown in Figure 2.3. Angle is calculated from the orientation data with respect to calibration.

The importance of sensor calibration to yield accurate measurements obtain from IMU sensors which in turn, makes good estimation of the motion possible. The calibration process is one of the steps to configure the sensor system for collecting motion.



Figure 2.3: T-pose for sensor calibration

2.4 Fusion Filters

Accelerometer, gyroscope and magnetometer have varying types of issues which are very limited when use separately. Furthermore, none of these sensor could be used to measure appropriate Earth fixed-frame orientation information. However, alternatives are available to combine this information and to correct mistakes using fusion filters.

Kalman Filter is an algorithm that measures previously and predicts next outcome, then fused with present measured information. It can be executed in real time, but it is more accurate, so it needs more calculation power (Matula, 2016). In Euler depiction, pitch and roll is predicted using accelerometers and gyroscope information, while the yaw is based on gyroscopes and magnetometers information. In Euler format, pitch and roll are usually measured using accelerometers and gyroscopes information (Paulich et al., 2018).

2.5 Conclusion

In this research, the application of Inertial Measurement Unit (IMU) sensors as motion tracking systems is most appropriate because of its ability to accurately track the desired motion. One of reasons is IMU sensors are able to communicate wirelessly and are suitable for lab-like environments and outdoor activities, which makes them suitable for application in unconstrained environments such as the plantation area. By using wireless communication, IMU sensors also does not restrict the movement of the workers. Last but not least, IMU sensors are light in weight so the sensors will not disturb the movement while performing the experiment.

Chapter 3: Methods

3.1 General Overview

The experiment was performed in a laboratory and data were collected from three subjects. The subjects were selected based on demographic information such as gender, age, physical ability and body size. All of the subjects were male and 23 years old. The subjects have no physical disabilities hence they were considered to be in good level of health.

The subjects were selected based on these demographic information because the intention was to resemble the actual demographic information for labours in plantation. However, the subjects had no working experience. However the activities are simple. The anthropometry measurement of the subjects are recorded in Table 1: Anthropometry measurement of the subjects. These information are used to determine the corresponding motion data of each respective sensors.

Anthropometry information	Anthropometry measurement (cm)		
	Subject Number 1	Subject Number 2	Subject Number 3
Height	167	172	165
Chest measurement	37	36	38
Arm length	45	50	47
Hand span	21	23	21
Front sleeve length	50	54	52
Leg length	90	95	92

Table 1: Anthropometry measurement of the subjects

The subjects are required to simulate the action of manual harvesting activities, namely calibration phase, lift up pole phase, tugging phase, lift down pole phase and recalibration phase

as shown in Figure 3.7 to Figure 3.11. The purpose of calibration activity is to align the IMU sensors orientation and to make sure the motion data conform to the real-time sensor orientation.

In addition, tugging activity was performed to replicate manual harvesting activity in the plantation. The subjects were required to repeat three times for tugging activities and also required to reach 3 meters height. The recalibration phase was required to validate the orientation of the IMU sensors after lift up, tugging and putting down the pole.

In this experiment, the subjects were required to wear the prototype exoskeleton. This upper limb exoskeleton is designed to support their right and left arms and the load from harvesting tools.

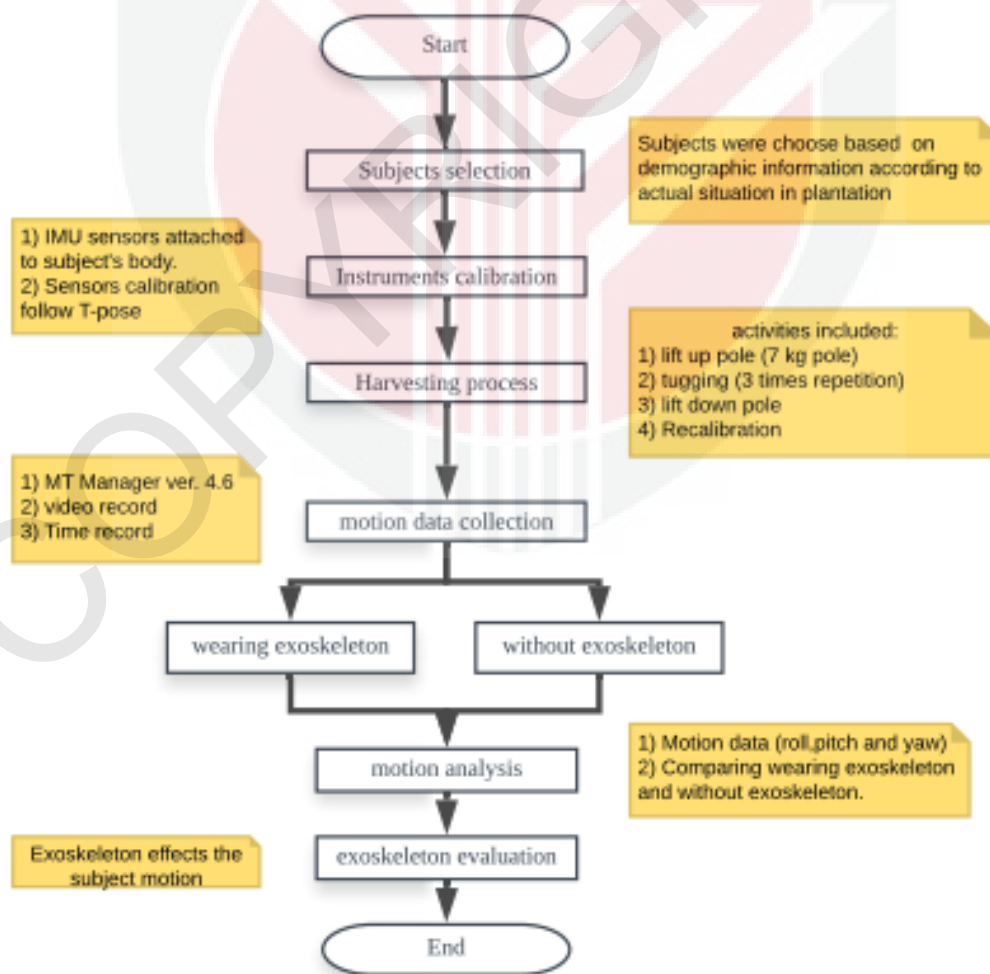


Figure 3.1: Summary of motion data acquisition in flowchart

3.2 Experimental Procedure

1. Each subjects had to wear IMU sensors which were placed at left scapula, right scapula, left humerus, right humerus, left radius, right radius, left metacarpal, right metacarpal and coccyx as shown in Figure 3.13.
2. All subjects were required to wear the exoskeleton and without exoskeleton and each subject was required to undergo manual harvesting activities. As shown in Figure 3.2 to Figure 3.7.
3. The activities included calibration phase, lift up pole phase, three times tugging phase, lift down pole phase and recalibration phase as shown in Figure 3.8 to Figure 3.12.
4. The subjects were required to carry a 7 kilograms pole when carry out harvesting activity. Motion data (roll, pitch and yaw) was recorded by using MT Manager version 4.6 Software. Additionally, the activities were record by a camera video to help determine the phase of an activity and also time of activities was recorded using timer trigger hardware.



Figure 3.2: Subject 1 without exoskeleton



Figure 3.3: Subject 1 wearing exoskeleton



Figure 3.4: Subject 2 without exoskeleton



Figure 3.5: Subject 2 wearing exoskeleton



Figure 3.6: Subject 3 without exoskeleton



Figure 3.7: Subject 3 wearing exoskeleton



Figure 3.8: Activity 1 (Calibration of sensors)



Figure 3.9: Activity 2 (Lift up pole)



Figure 3.10: Activity 3 (Tugging)

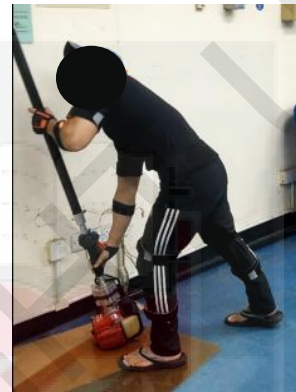


Figure 3.11: Activity 4 (Lift down pole)

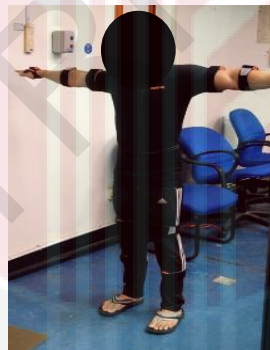


Figure 3.12: Activity 5 (Recalibration)

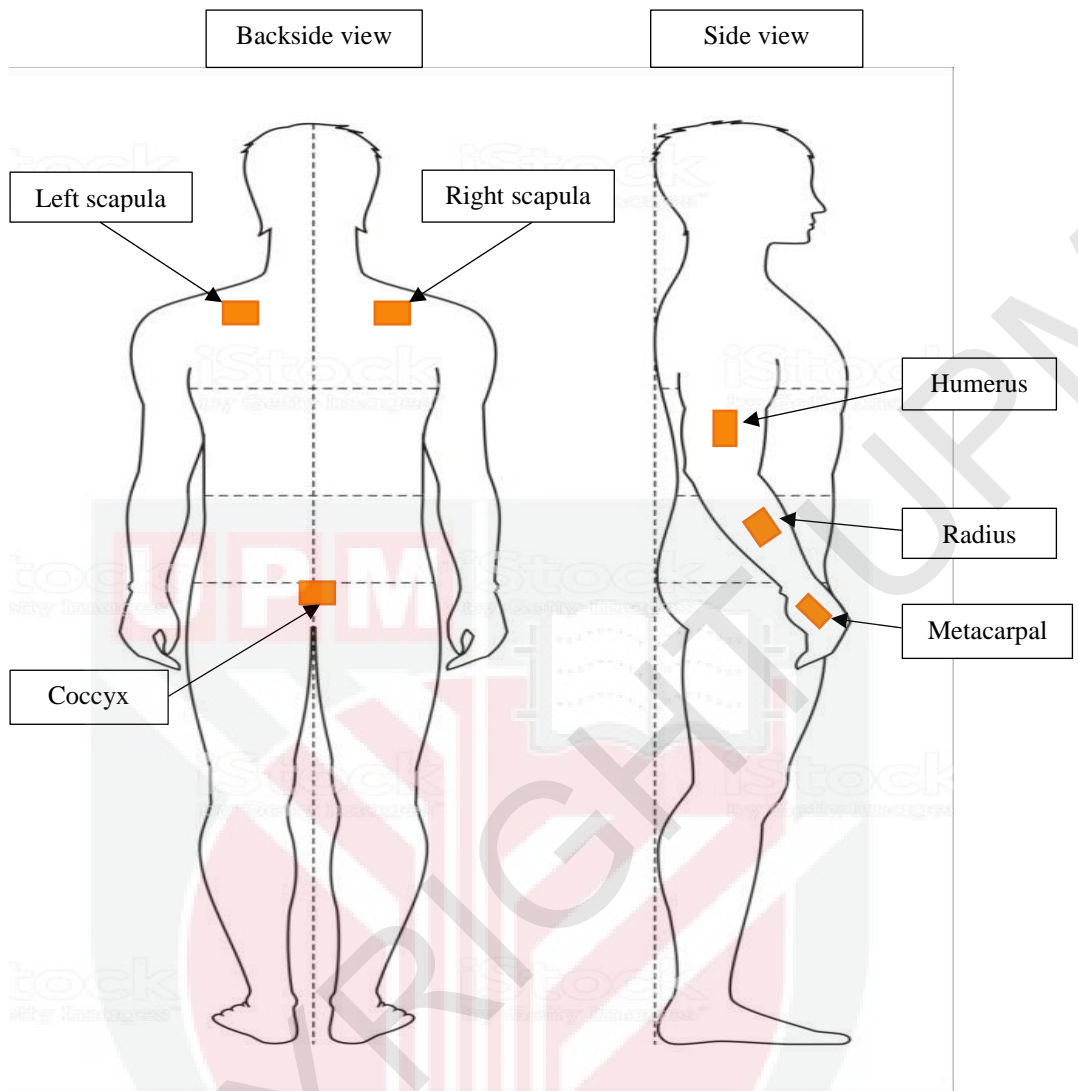


Figure 3.13: Illustration of IMU sensors location at subject's limbs

Legends:
 ■; IMU sensors

Chapter 4: Results and Discussion

4.1 IMU Sensor Calibration and Orientation

From Figure 2.1, the term of roll in motion data refers to rotation of an IMU sensor at x-axis, pitch refers to rotation of an IMU sensor at y-axis and yaw refers to rotation of an IMU at z-axis. While angle of motion (measured in Degree) which is shown at horizontal axis in every graph indicates the rotation of the body limbs with respect to the rotation the IMU sensors at x, y and z-axis. From there, we able to plot the motion data (roll, pitch and yaw) for respective body limbs.

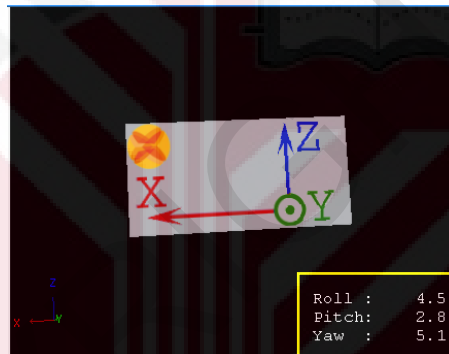


Figure 4.1: Orientation of sensor when motion data is near to $(0^\circ, 0^\circ, 0^\circ)$

The sign when the sensors are properly calibrated is the display of the axis for all sensors shows similarity. For example, the x-axis of all IMU sensors at upper limb (referred to Figure 3.13) should pointing from left to right, y-axis should will pointing to front and z-axis will pointing upward. However, the sensors may be display different orientation depending the location of IMU sensor at body. Thus, bring to another sign for properly calibrated sensor which the displayed orientation of IMU sensors should follow the real time orientation of the sensors at the body. Taking example motion data sensor at coccyx, the roll motion data (referred Figure 4.8) shows the initial status reading is 70° which the IMU sensor at coccyx are tilted at x-axis. Ultimately, the proper sensors calibration will display the real time orientation

of sensors. For example, Figure 4.1 shows the orientation of sensor when the IMU sensor at right humerus properly calibrated so motion data is near to $(0^\circ, 0^\circ, 0^\circ)$ and also display the real time IMU orientation.

From Figure 4.2 to Figure 4.7, we able to see the IMU sensor orientation for positive and negative roll motion data, positive and negative pitch motion data and positive and negative yaw motion data. Noted that, when sensors rotates clockwise; the motion data will be represent in positive values and vice versa. Also, these figures are to define the orientation of an IMU at right radius (referred Figure 3.13).

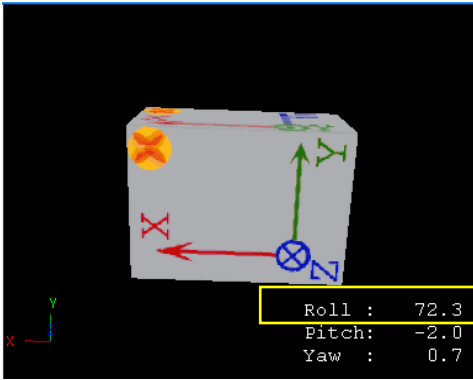


Figure 4.2: IMU sensor orientation when roll motion data is positive

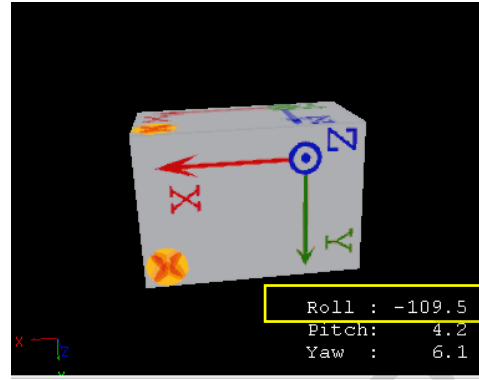


Figure 4.3: IMU sensor orientation when roll motion data is negative

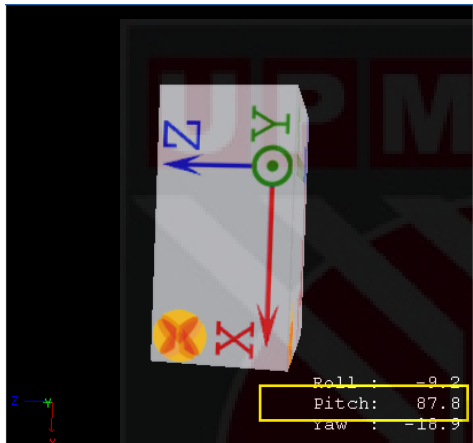


Figure 4.4: IMU sensor orientation when pitch motion data is positive

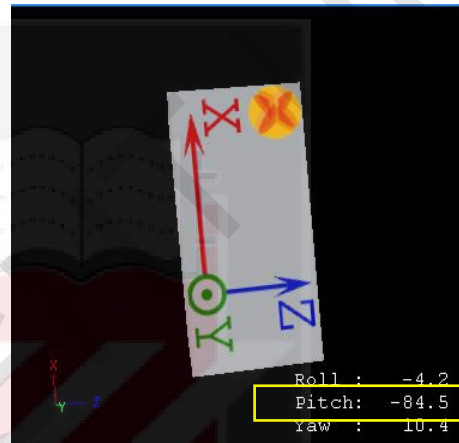


Figure 4.5: IMU sensor orientation when pitch motion data is negative



Figure 4.6: IMU sensor orientation when yaw motion data is positive

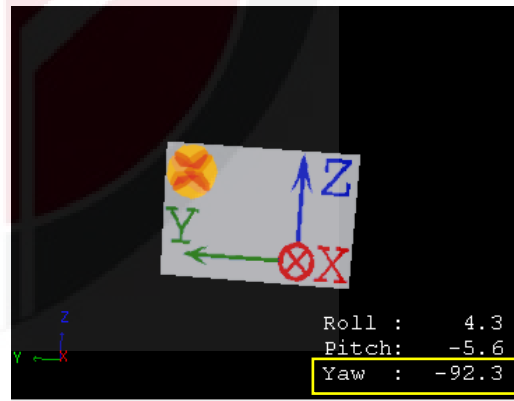


Figure 4.7: IMU sensor orientation when yaw motion data is negative

4.2 Impact of the Exoskeleton toward motion of limbs

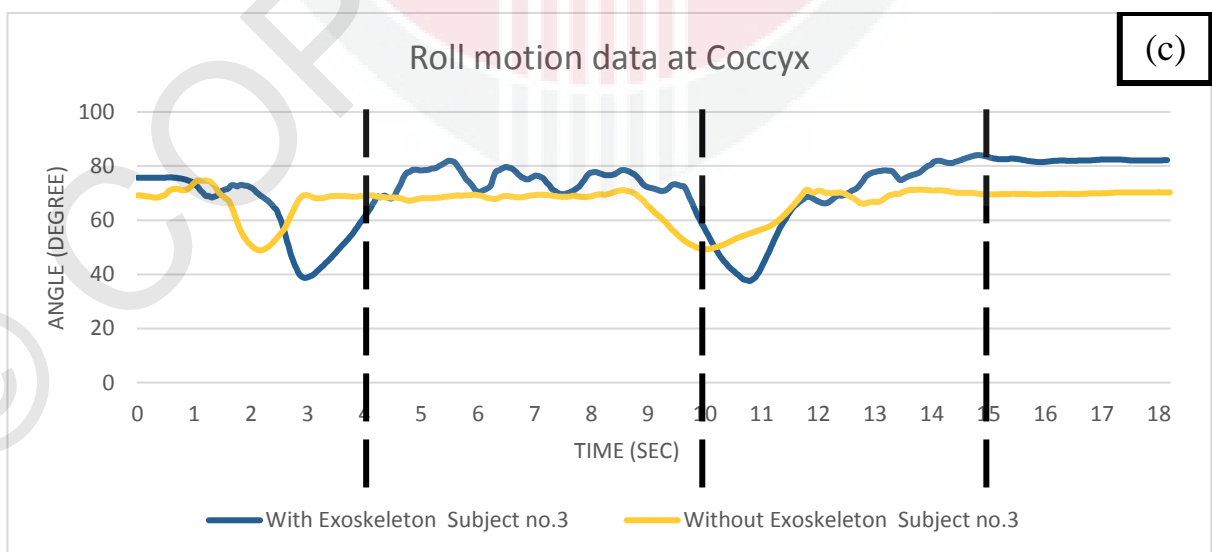
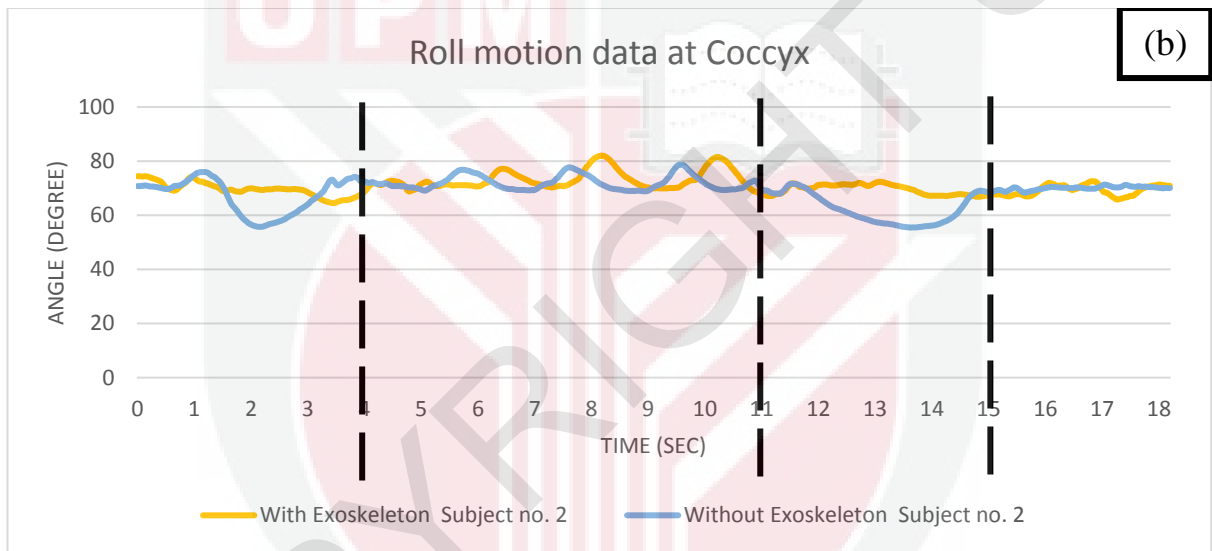
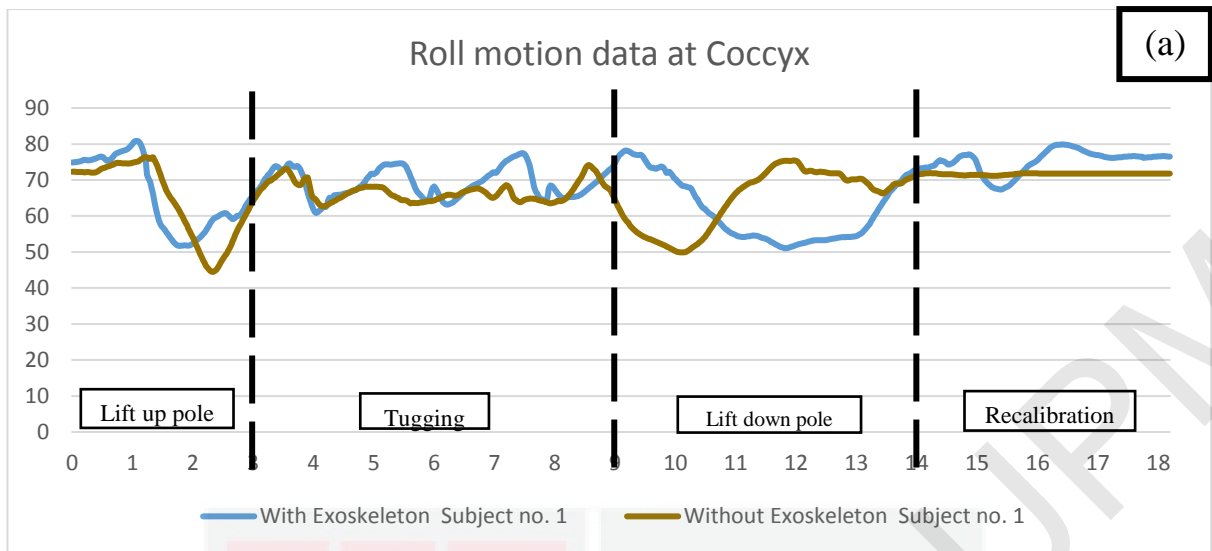


Figure 4.8: Graphs for roll motion data at coccyx. (a) Subject number 1. (b) Subject number 2. (c) Subject number 3.

Figure 4.8 shows the roll motion data at coccyx (referred in Figure 4.9) and this data are to determine the lower body flexion and extension. In Figure 4.8(a), Figure 4.8(b) and Figure 4.8(c) shows graphs when wearing exoskeleton for subject number 1, 2 and 3. During lift up pole and lift down pole for all of subjects show lower degrees of motion comparing not wearing exoskeleton. By calculating differences of motion angle when wearing and not wearing exoskeleton for all subjects during lift up pole and lift down pole graphs, we able to identify graph in Figure 4.8 when subject wearing exoskeleton show lower angle drop compare to not wearing exoskeleton. This is because the subjects flexed their body forward when reaching and put down the pole (as shown in Figure 3.9 and Figure 3.11) but not as low as not wearing exoskeleton. Also, the graphs in Figure 4.8 show one second delay when the subjects wearing exoskeleton. From here, we can see that the exoskeleton imposed some movement restriction on the subjects' lower body.

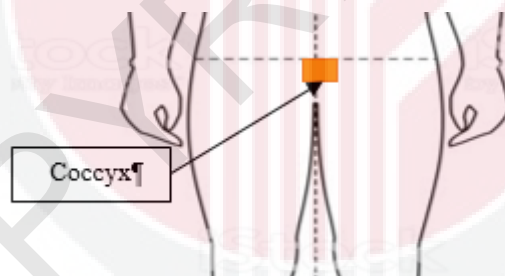


Figure 4.9: Location of an IMU sensor at coccyx

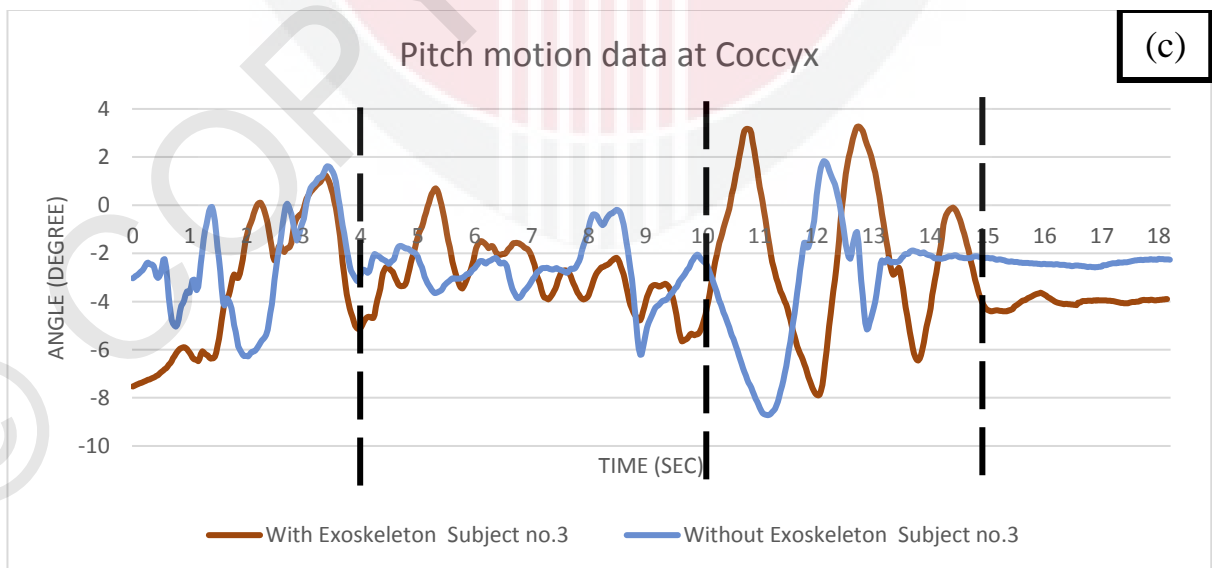
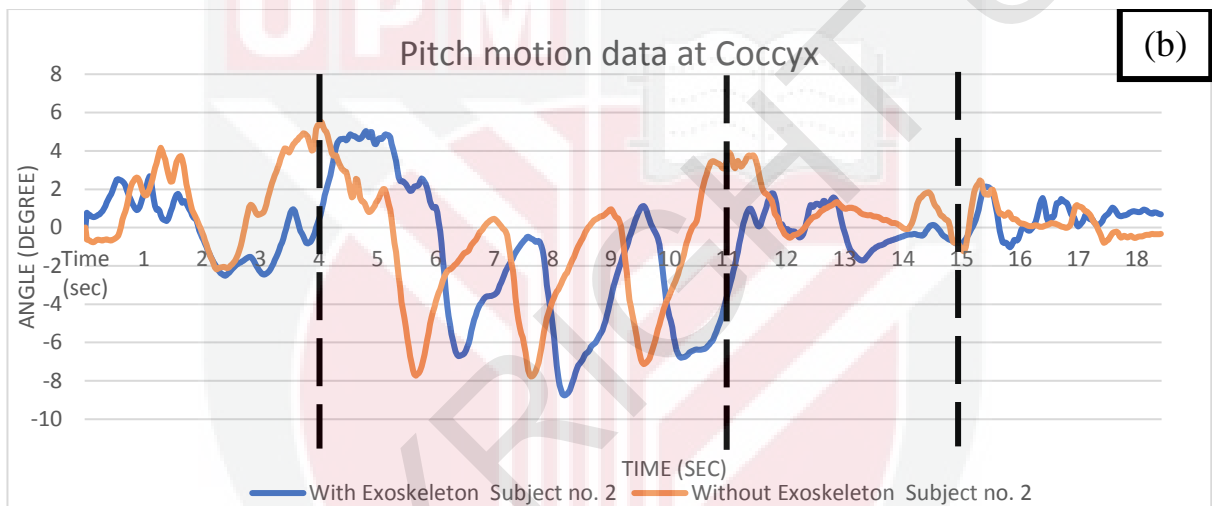
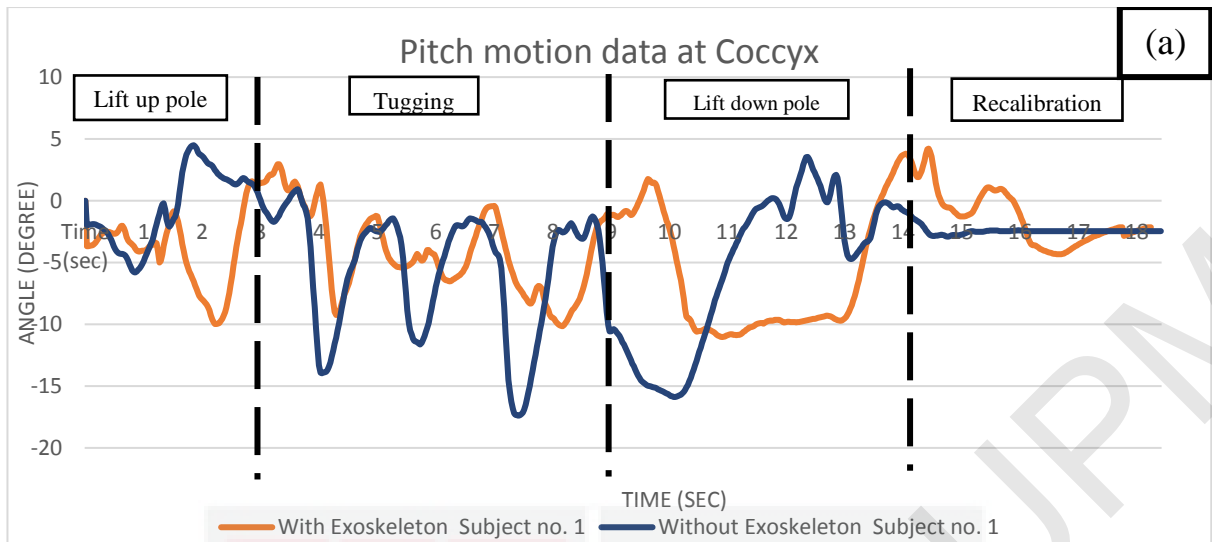


Figure 4.10: Graphs for pitch motion data at coccyx. (a) Subject number 1. (b) Subject number 2. (c) Subject number 3.

Figure 4.10: Graphs for pitch motion data at coccyx. (a) Subject number 1. (b) Subject number 2. (c) Subject number 3. When focusing at tugging activity in Figure 4.10 (a), we can see that there are amplitude differences for subject no.1 compared to other subjects. Subject no.1 shows larger differences in average, while subject no.2 and no.3 show less differences in average in angle of motion. Noted that pitch at coccyx in Figure 4.10 is to determine the lower body's rotation. Figure 4.10 (a) shows that when wearing exoskeleton, the body of subject no.1 rotates to the left but less compared to not wearing the exoskeleton. However, the situation is not the same for subject no.2 (Figure 4.10 (b)) and no.3 (Figure 4.10 (c)) as their lower body rotation is not affected by wearing exoskeleton. This shows that wearing exoskeleton gives an advantage in order to prevent musculoskeletal system diseases as there is restriction towards the body rotation.

While in lift down pole activity from Figure 4.10, the graphs for all subjects show different trends. But actually the graphs want to show that subject's body rotation when put down the pole. For subject no.1 and no.2, when wearing exoskeleton shows less rotation than when not wearing exoskeleton. However, exoskeleton does not impose restriction on subject no. 3's body rotation.

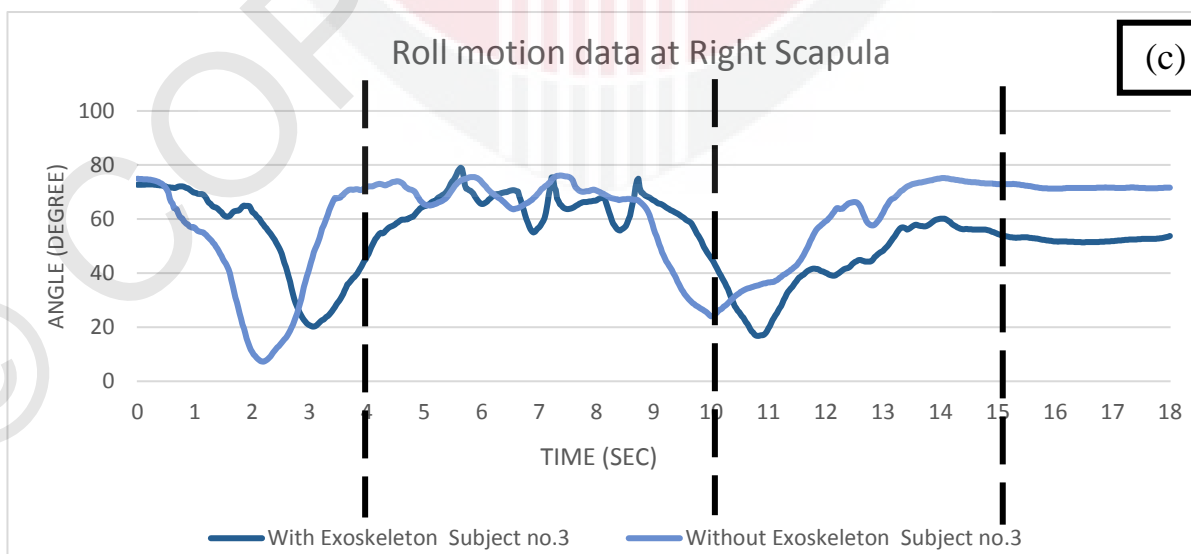
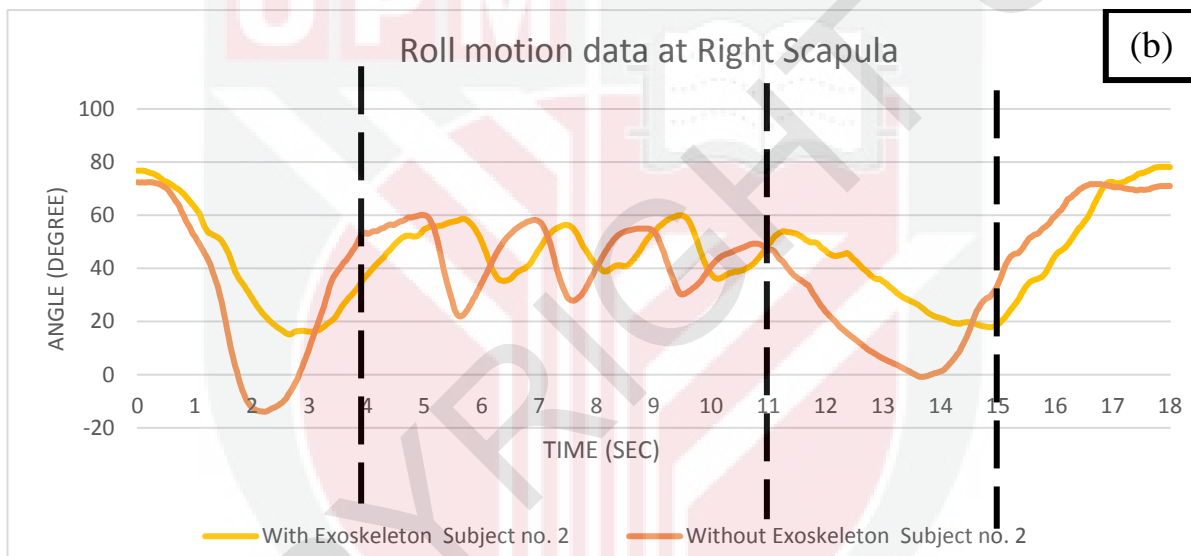
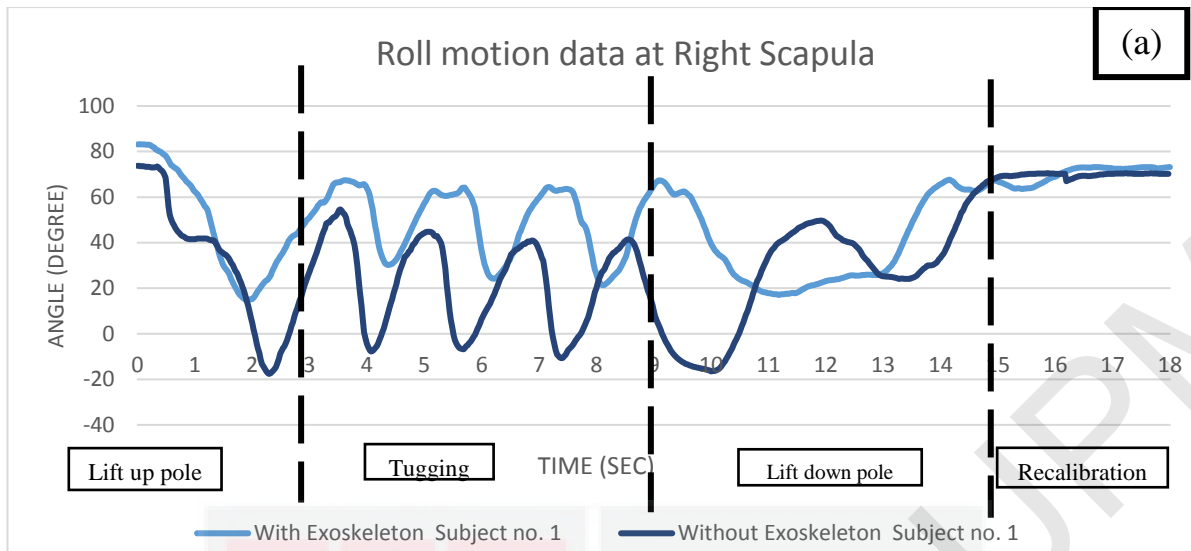


Figure 4.11: Graphs for roll motion data at right scapula. (a) Subject number 1. (b) Subject number 2. (c) Subject number 3.

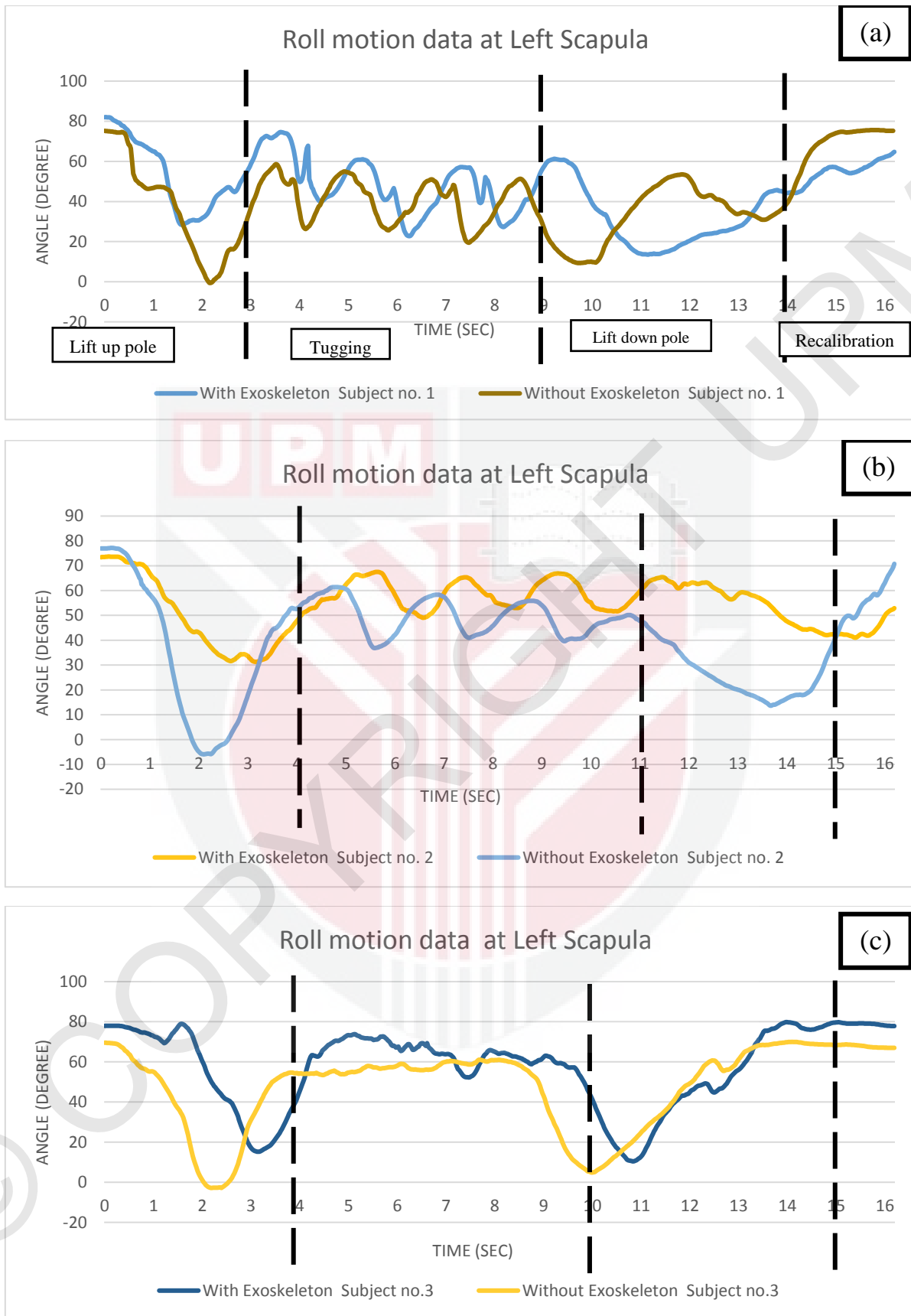


Figure 4.12: Graphs for roll motion data at left scapula. (a) Subject number 1. (b) Subject number 2. (c) Subject number 3.

Figure 4.11: Graphs for roll motion data at right scapula. (a) Subject number 1. (b) Subject number 2. (c) Subject number 3. Figure 4.12: Graphs for roll motion data at left scapula. (a) Subject number 1. (b) Subject number 2. (c) Subject number 3. As we able to measure roll motion data at scapula (Figure 4.11 and Figure 4.12), so now we able to determine the forward and backward movement of upper body. By comparing roll motion graph between left and right scapula for all subjects during lifting and put down the pole, we able to see the graphs shows similar trend. The graphs show that the subjects will bow with lower angle when wearing exoskeleton. This result shows that exoskeleton will improve the subjects' body posture and prevent over flexion of the subject's backbone.

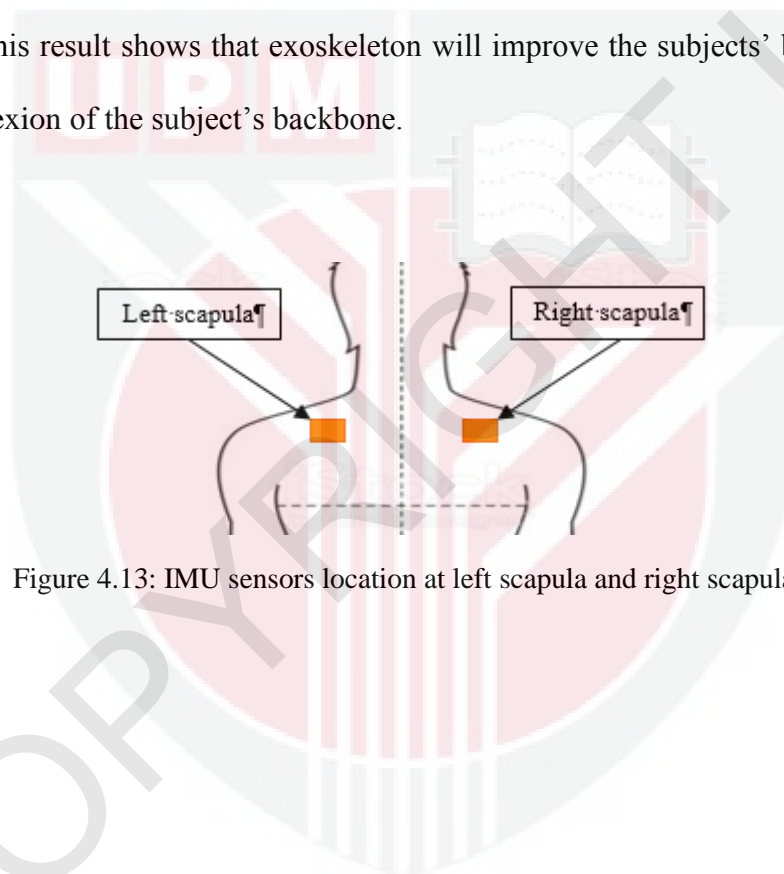


Figure 4.13: IMU sensors location at left scapula and right scapula

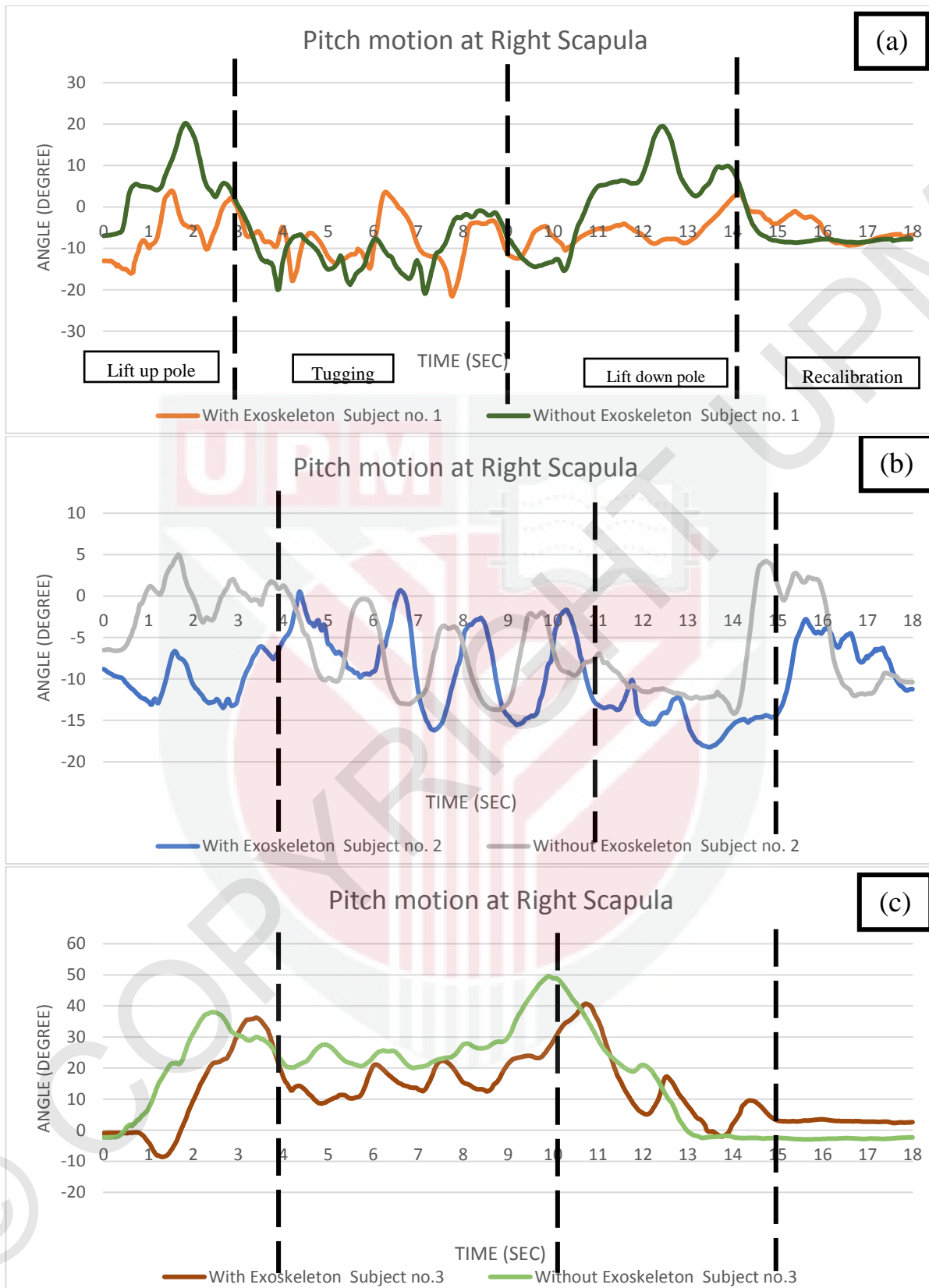


Figure 4.14: Graphs for pitch motion data at right scapula. (a) Subject number 1. (b) Subject number 2. (c) Subject number 3.

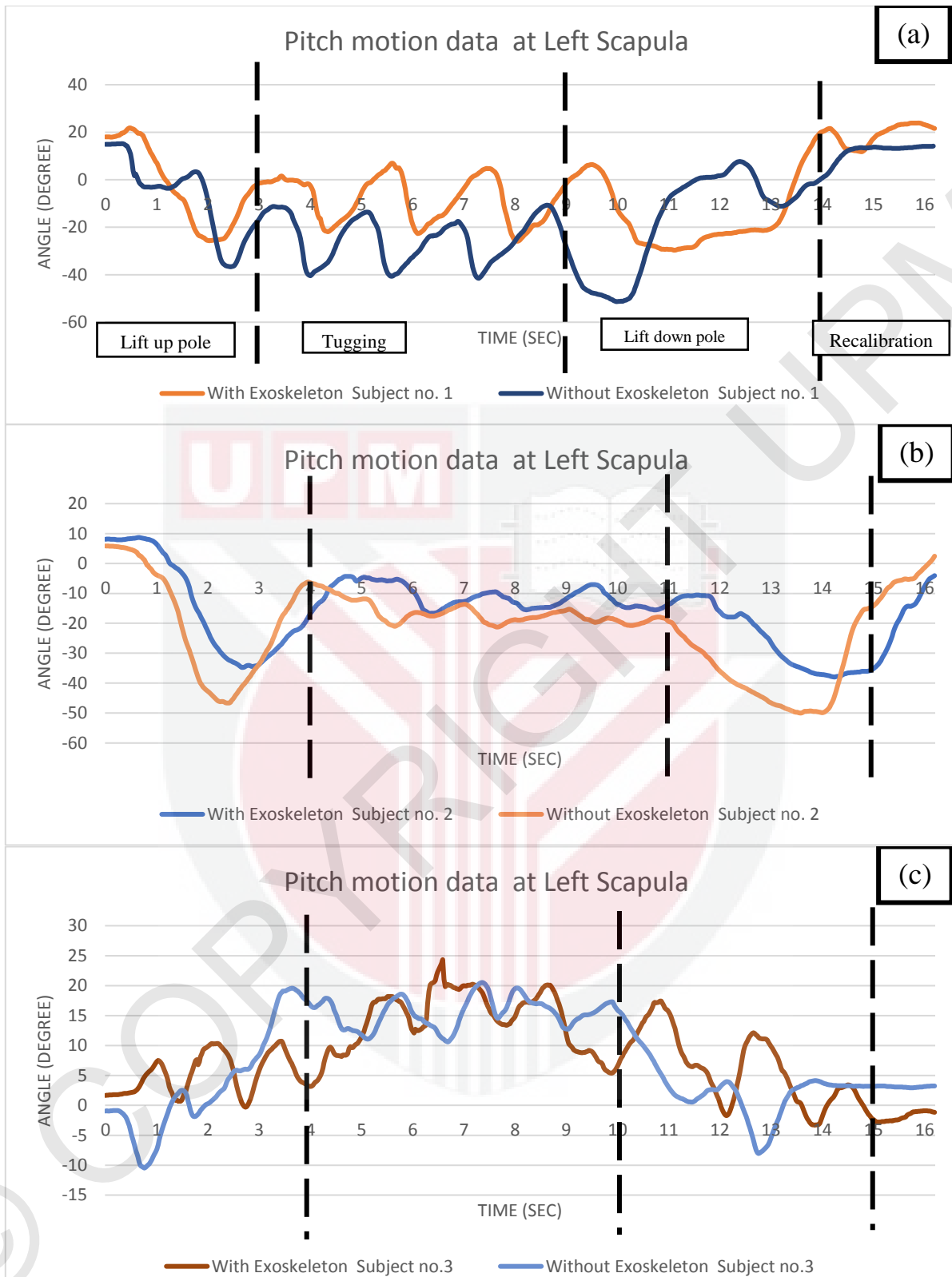


Figure 4.15: Graphs for pitch motion data at left scapula. (a) Subject number 1. (b) Subject number 2. (c) Subject number 3.

Figure 4.14 shows graphs from pitch motion data at right scapula and Figure 4.15 shows graphs from pitch motion data at left scapula. From pitch motion data at scapula as shown in Figure 4.14 and Figure 4.15, we can estimate the upper body rotation. The graphs in Figure 4.14 and Figure 4.15 show that exoskeleton does not have significant effect on the upper body rotation for tugging activity. However, there are significant time delay for motion data when wearing exoskeleton. This can be describe that exoskeleton does slow down the subject movements.



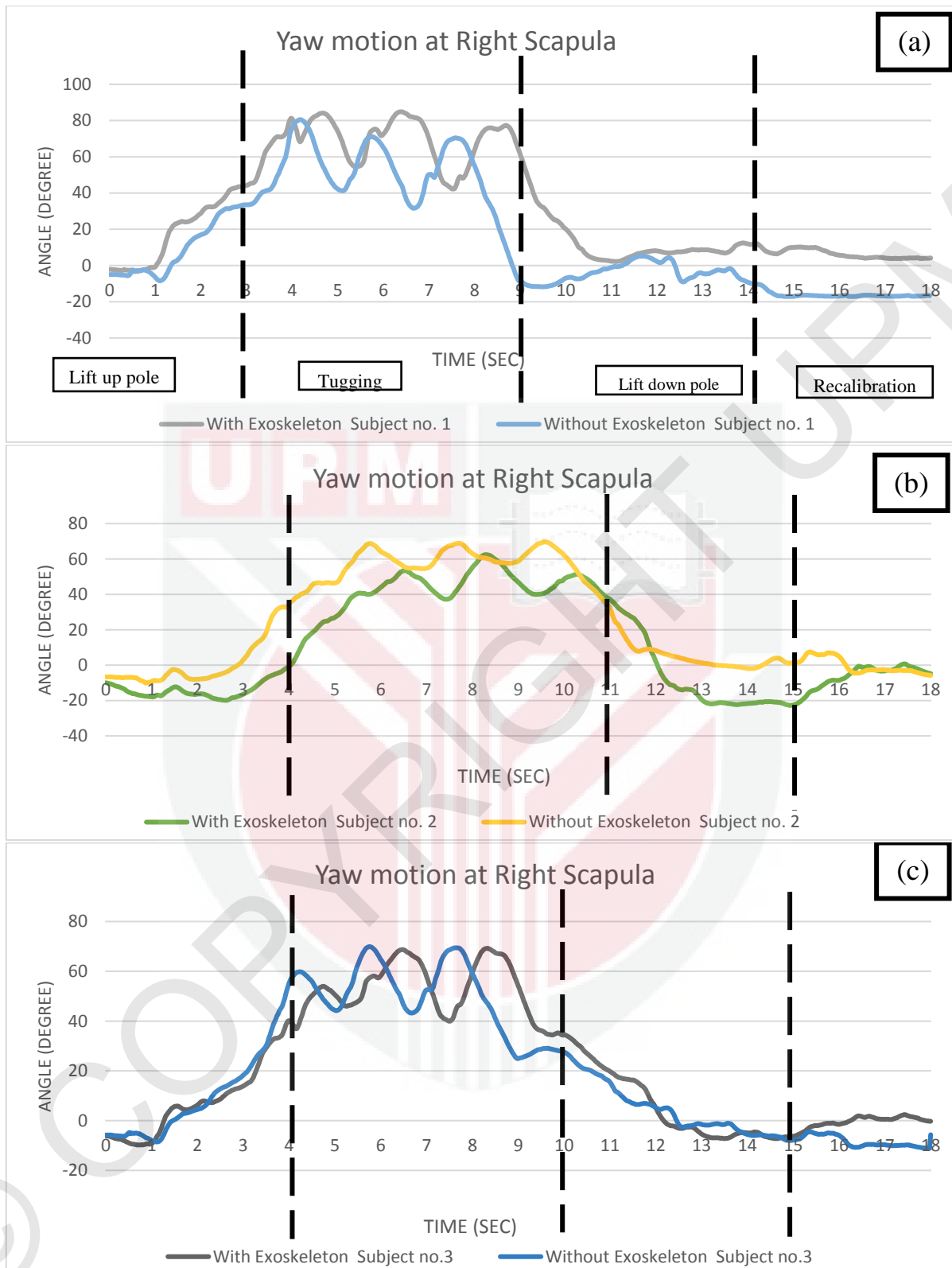


Figure 4.16: Graphs for yaw motion data at right scapula. (a) Subject number 1. (b) Subject number 2. (c) Subject number 3.

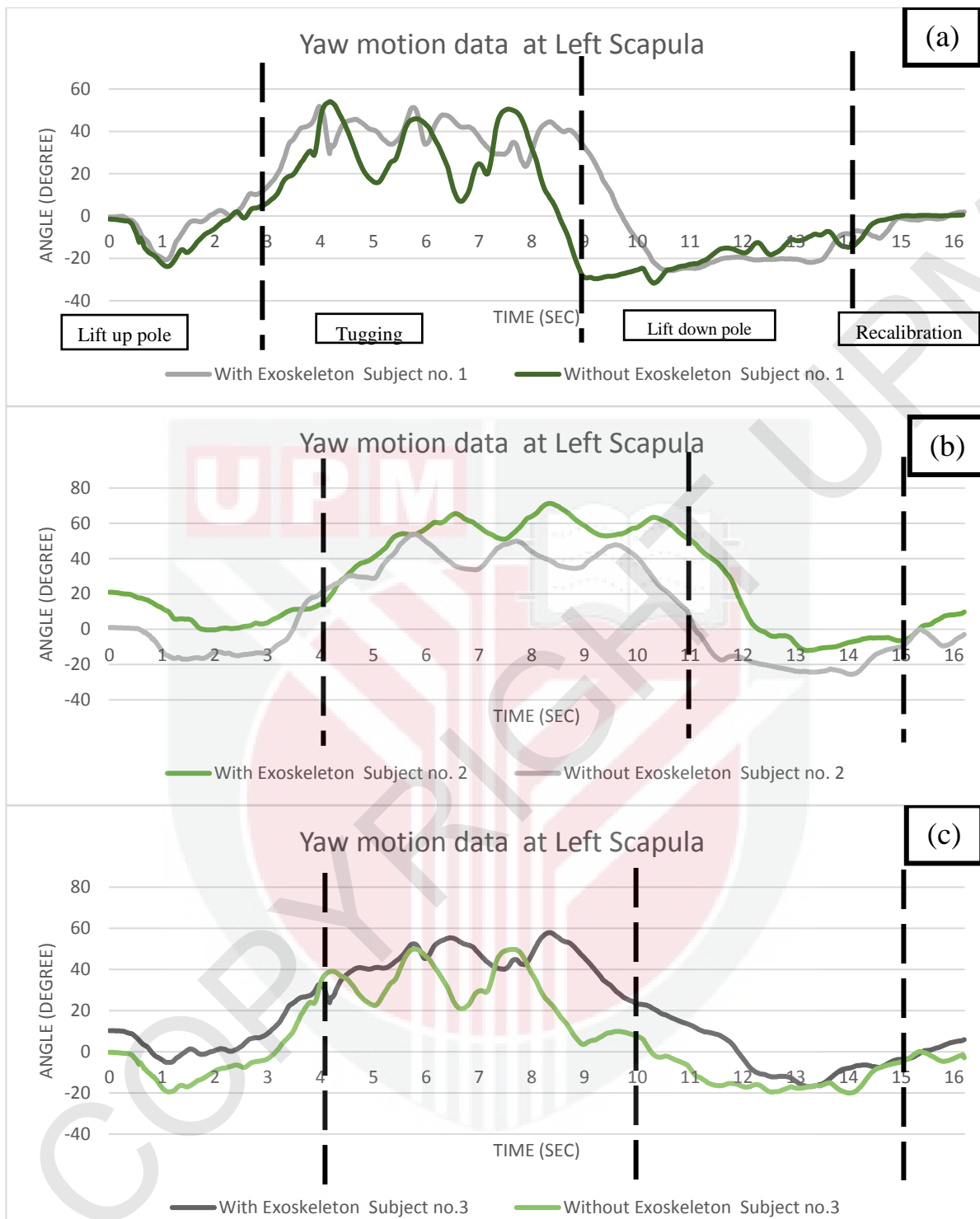


Figure 4.17: Graphs for yaw motion data at left scapula. (a) Subject number 1. (b) Subject number 2. (c) Subject number 3.

Figure 4.16 show graphs for yaw motion data at right scapula and Figure 4.17 show graphs for yaw motion data at left scapula. From yaw motion data at scapula (Figure 4.13), we can estimate the upper body tilt. The graphs show that exoskeleton does not gives significant effect on the upper body tilts for harvesting activity. However, there are significant time delay for motion data when wearing exoskeleton. This can be describe that exoskeleton does slow down the subject movements.



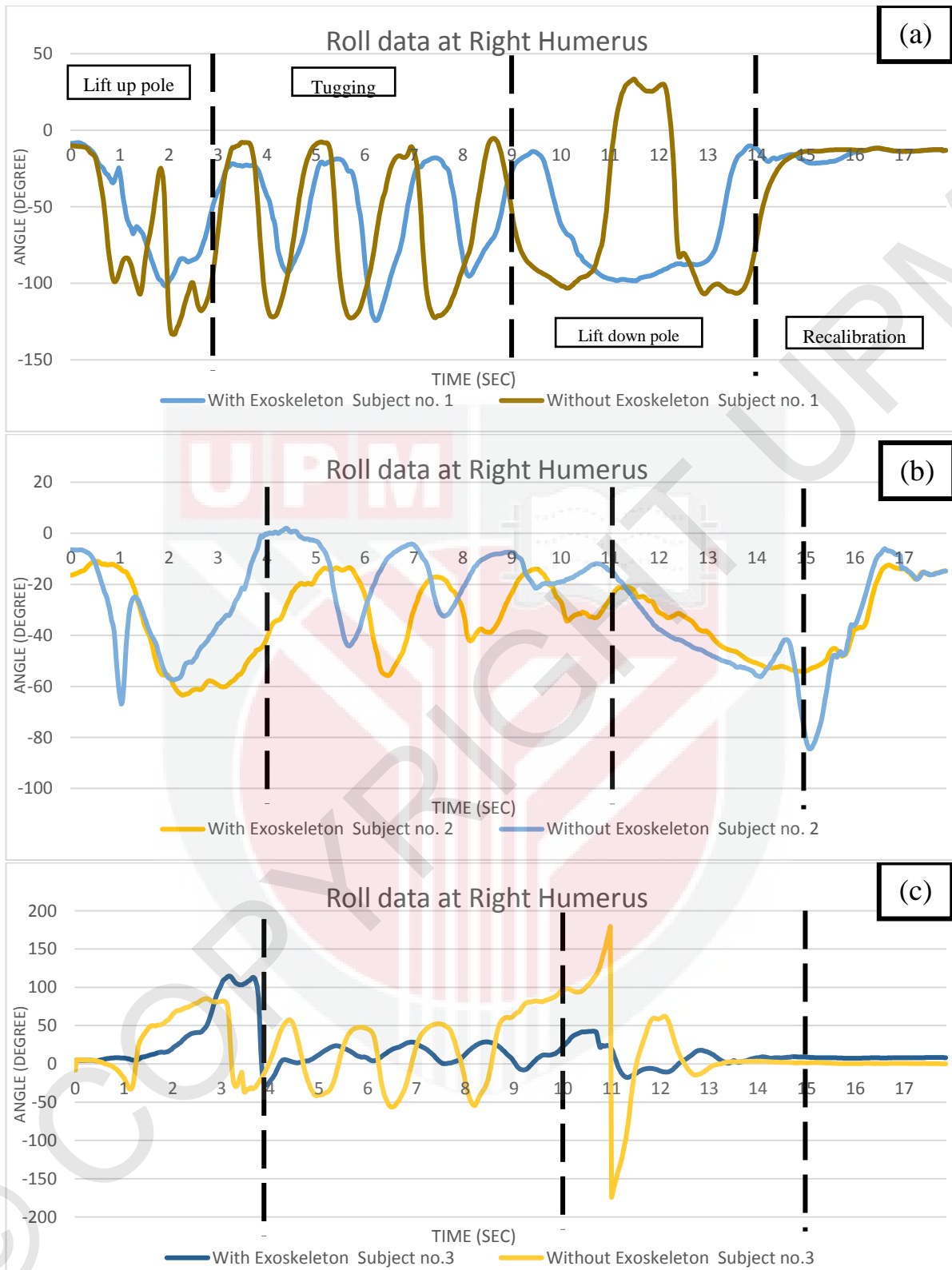


Figure 4.18: Graphs for roll motion data at right humerus. (a) Subject number 1. (b) Subject number 2. (c) Subject number 3.

Figure 4.18 show graphs for roll motion data at right humerus. By looking for all activities, subjects' right humerus (Figure 4.18(a), (b) and (c)) show less rotation at x-axis when wearing the exoskeleton. During tugging activity, the graphs show that there is small amplitude changes when comparing wearing and not wearing exoskeleton. The graphs for wearing exoskeleton have smaller angle of motion. This mean that exoskeleton impose restriction to muscle on roll motion at right. However, this restriction are beneficial to the subjects because will helps to prevent muscle soreness. Similarly in lift down pole activity, when wearing exoskeleton, right humerus not rotate as much as not wearing exoskeleton.

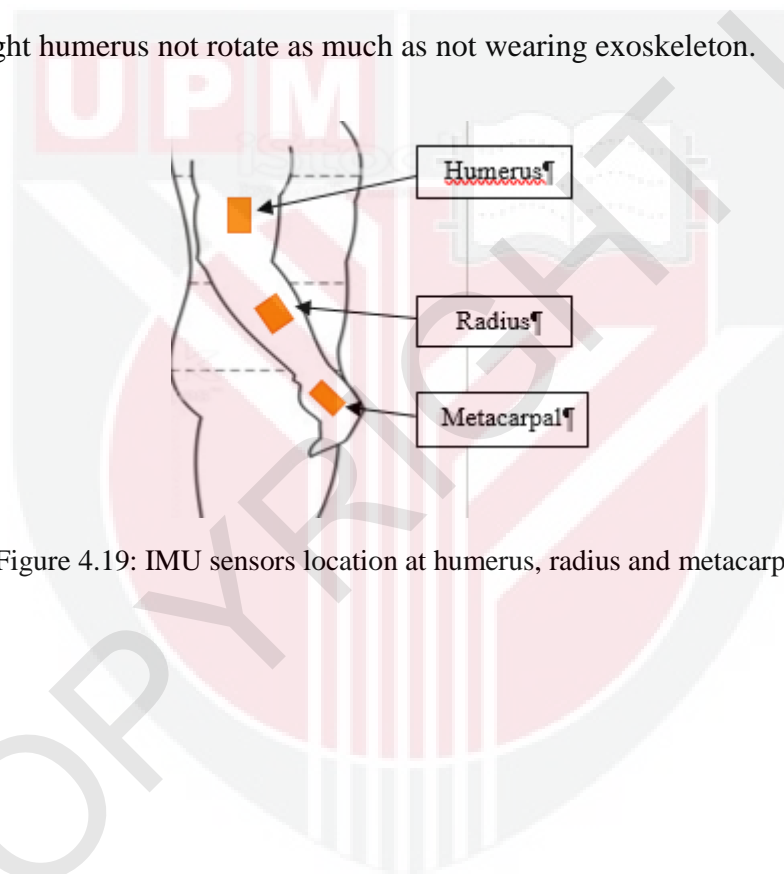


Figure 4.19: IMU sensors location at humerus, radius and metacarpal.

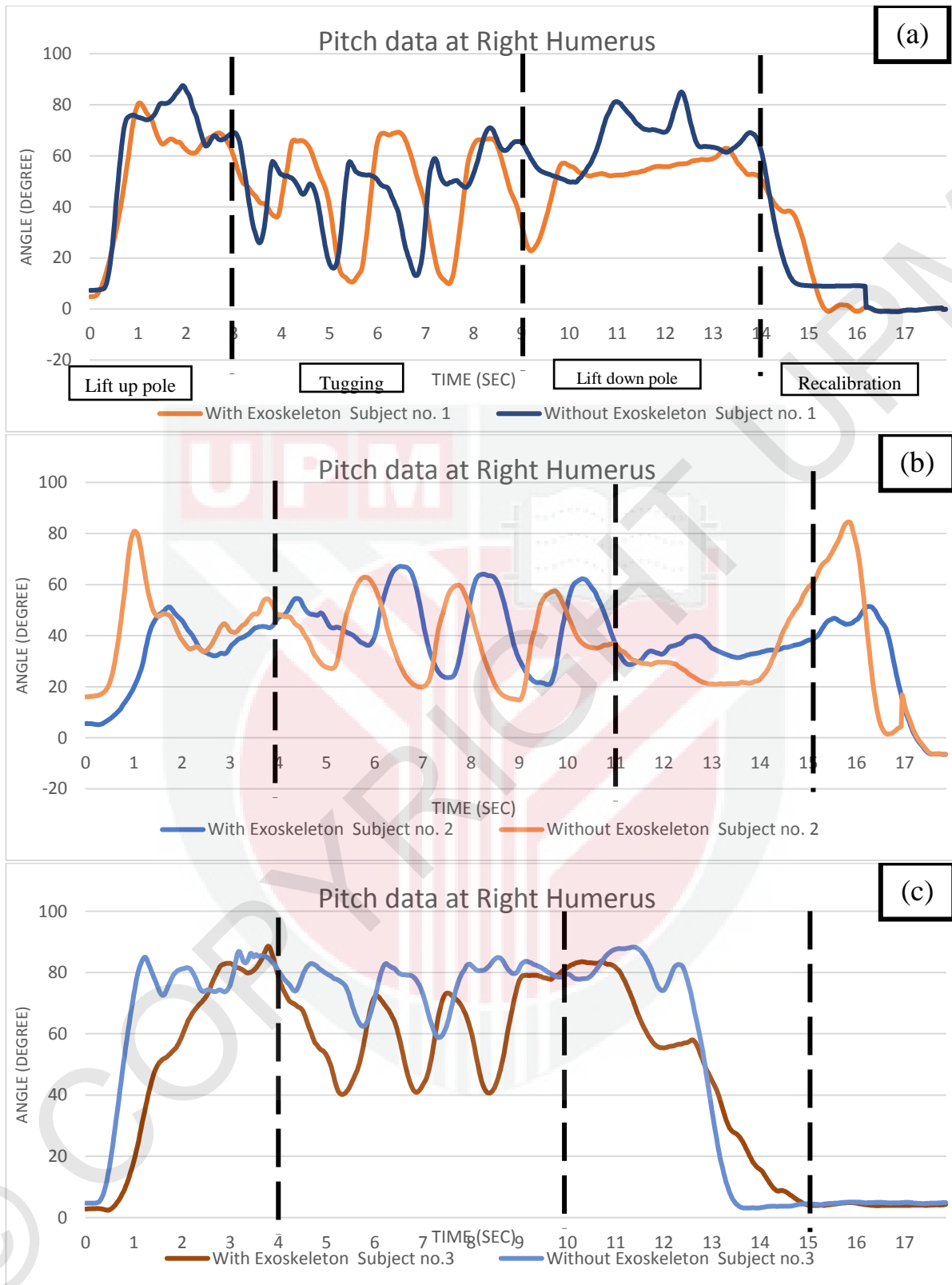


Figure 4.20: Graphs for pitch motion data at right humerus. (a) Subject number 1. (b) Subject number 2. (c) Subject number 3.

Figure 4.20 show graphs for pitch motion data at right humerus. In tugging activity, pitch motion graphs for wearing exoskeleton from all subjects (Figure 4.20(a), (b) and (c)) show larger amplitudes compared to not wearing exoskeleton. The reason is because the subjects need to give extra forces when tugging. The forces are applied to against the force exerted from spring under the right humerus. Due to the extra forces, the subjects create higher inertia at right humerus and give larger angle pitch motion.



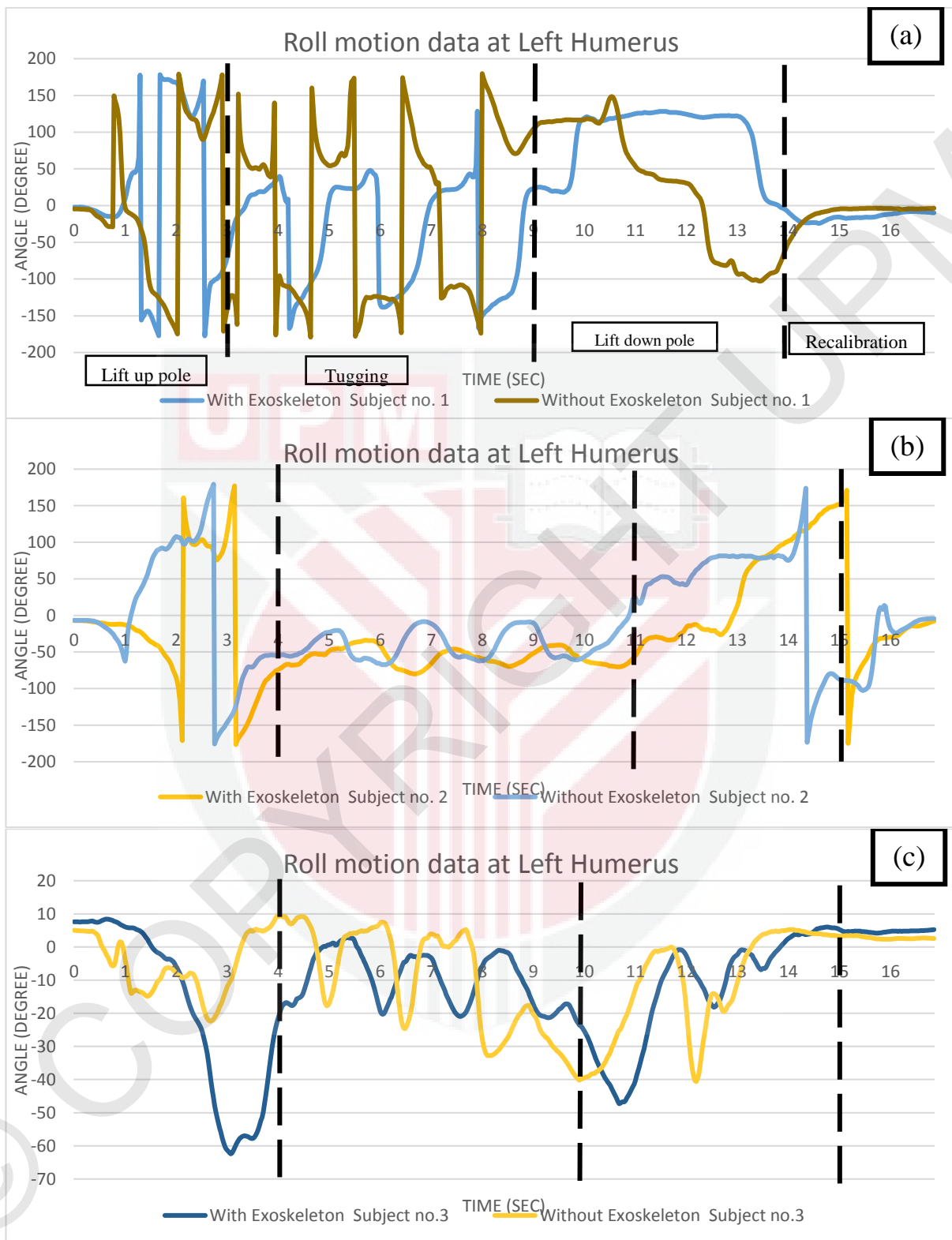


Figure 4.21: Graphs for roll motion data at left humerus. (a) Subject number 1. (b) Subject number 2. (c) Subject number 3.

Figure 4.21 show graphs for roll motion data at left humerus. During lift up pole activity, subject number 1 (Figure 4.21(a)) and 2 (Figure 4.21 (b)) show similar graph pattern for both wearing and not wearing exoskeleton. This shows that left humerus of both subject circumduction vigorously either wearing or not wearing exoskeleton. However, graphs for subject number 3 (Figure 4.21(c)) shows different pattern roll motion pattern as the left humerus shows steady drop of angle. This is because left humerus of subject number 3 rotated steadily on x-axis.

While in tugging activity, subject number 1 (Figure 4.21(a)) shows many spikes for both wearing and not wearing exoskeleton graphs. However, in the graph for not wearing exoskeleton show larger angle of motion compared to not wearing exoskeleton. In this activity, subject number 1 (Figure 4.21(a)) moves his left humerus circumduction (Figure 4.22) vigorously when not wearing exoskeleton. When wearing exoskeleton, the angle of motion is been reduced and this is beneficial to prevent muscle soreness and injury.

However, subject number 2 (Figure 4.21 (b)) and 3 (Figure 4.21 (c)) show no spike for both wearing and not wearing exoskeleton. This means that the subjects' limb did not make sudden rotation at x-axis. But, the graph for wearing exoskeleton shows lower angle of motion compared to not wearing exoskeleton. Which bring advantages in preventing muscle soreness.

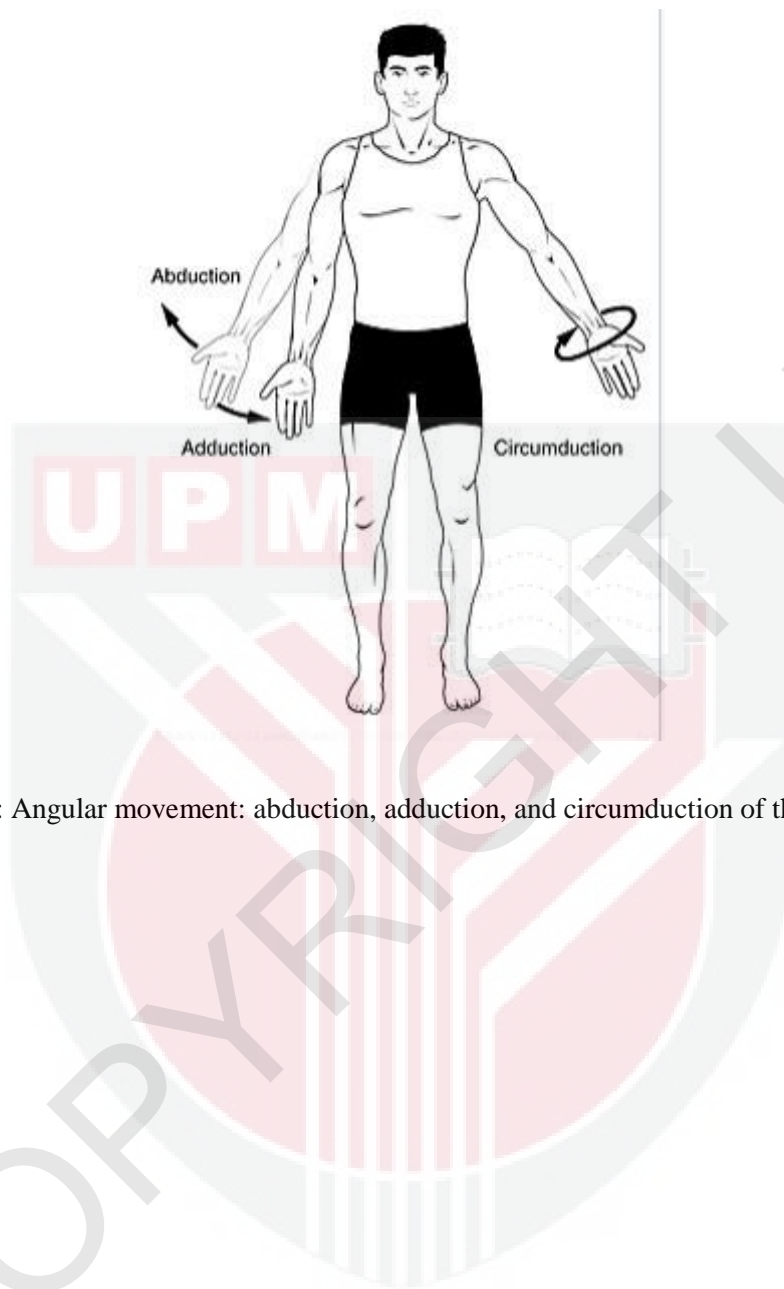


Figure 4.22: Angular movement: abduction, adduction, and circumduction of the upper limb

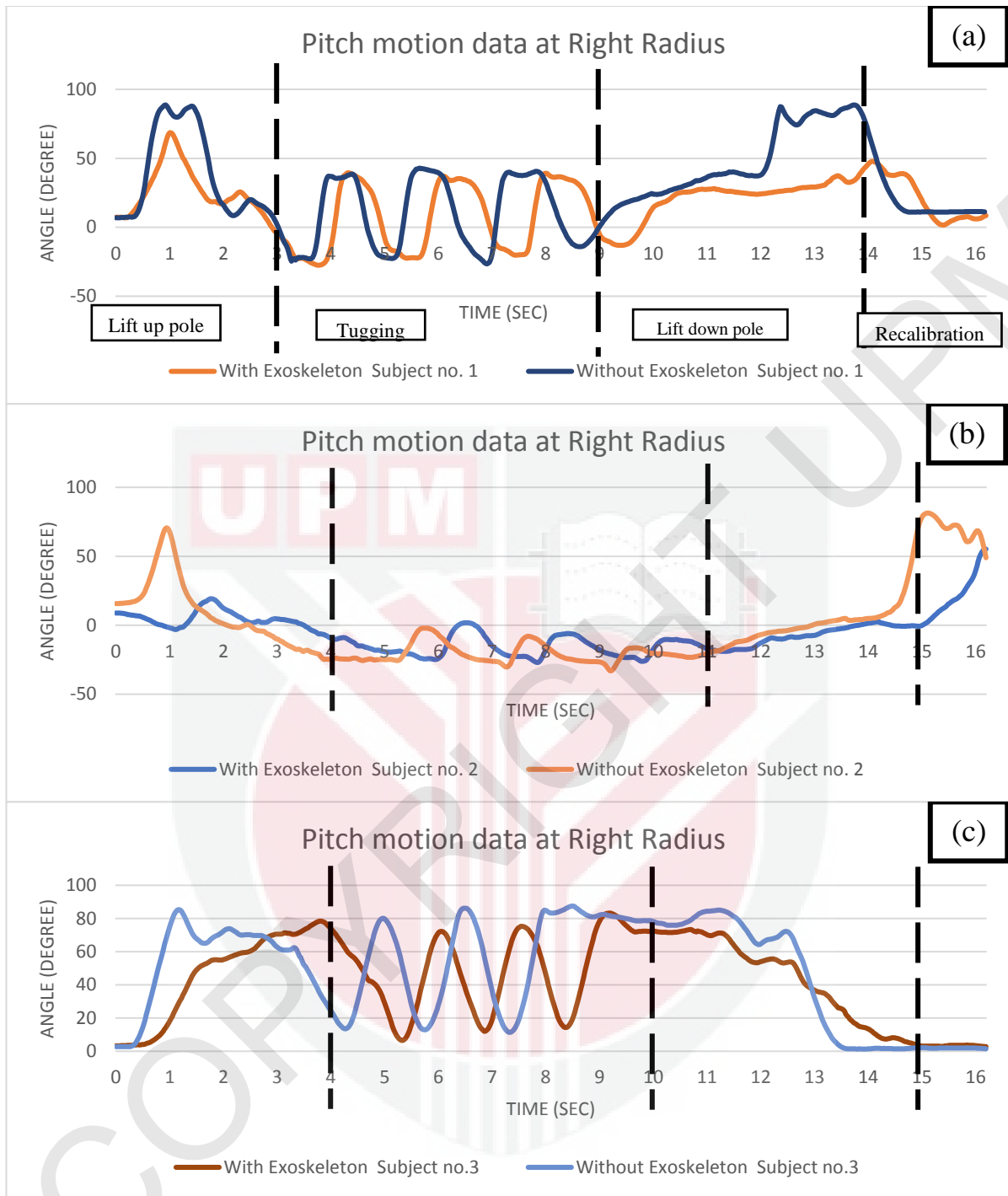


Figure 4.23: Graphs for pitch motion data at right radius. (a) Subject number 1. (b) Subject number 2. (c) Subject number 3.

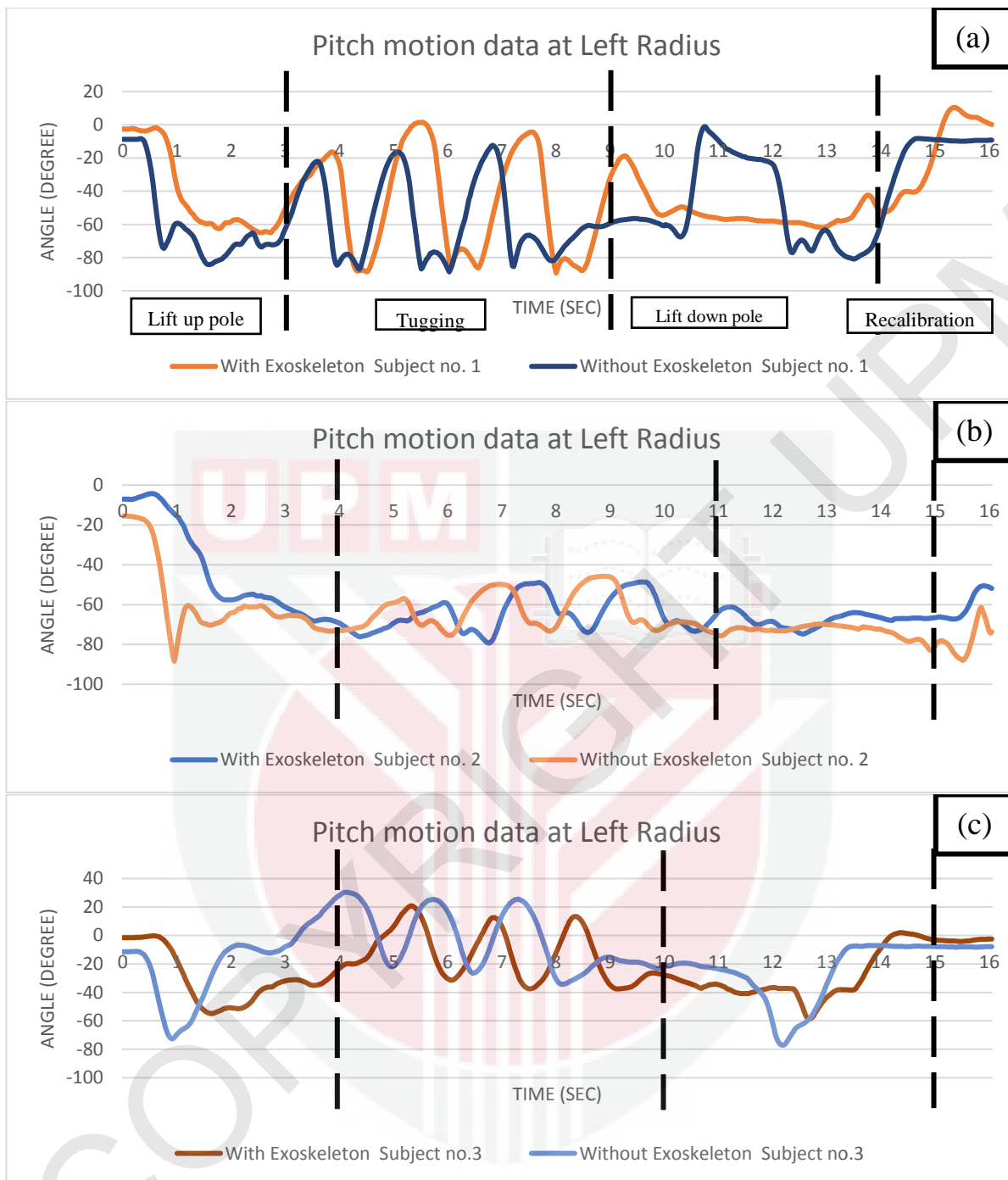


Figure 4.24: Graphs for pitch motion data at left radius. (a) Subject number 1. (b) Subject number 2. (c) Subject number 3.

Figure 4.23 show graphs for pitch motion data at right radius. Figure 4.24 show graphs for pitch motion data at left radius. Pitch motion data from the graphs will help to determine abduction and adduction for right and left radius. When refer at graphs for pitch motion data at right and left radius, we can see that the graphs for all subjects (Figure 4.23 (a), (b), (c) and Figure 4.24 (a), (b), (c)) when wearing exoskeleton during lift up pole and lift down pole show lower angle of motion. The reason for smaller angle of adduction (Figure 4.22) for right and left radius when wearing exoskeleton is because the radius movement was restricted by exoskeleton but at the same time the exoskeleton support the radius as shown in Figure 4.25.

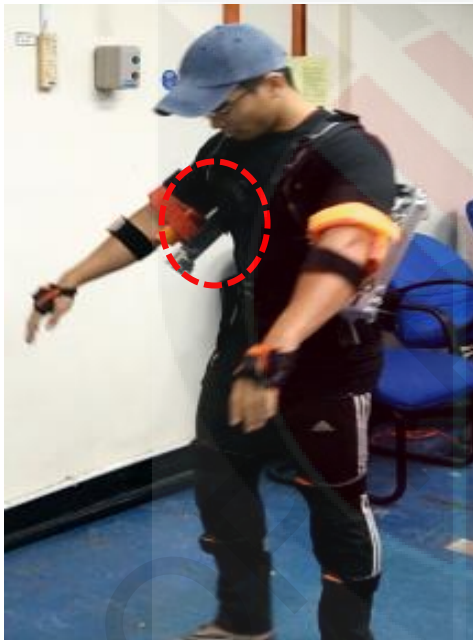


Figure 4.25: Adduction when wearing exoskeleton

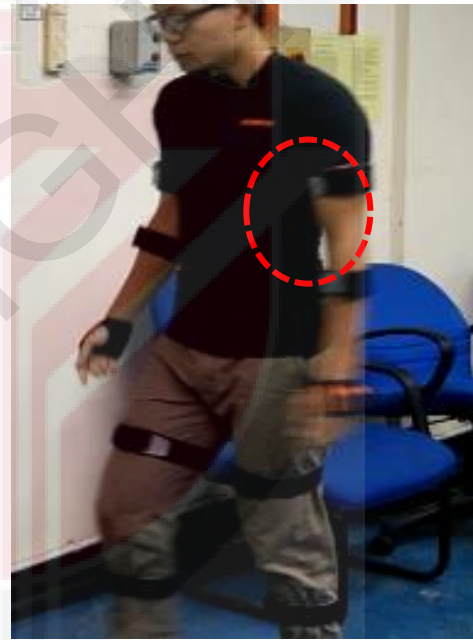


Figure 4.26: Adduction when not wearing exoskeleton

However, the graphs for wearing exoskeleton during tugging activity shows similar trend and amplitudes comparing with not wearing exoskeleton. This is because exoskeleton did not impose restriction on the movement of radius during tugging activity.

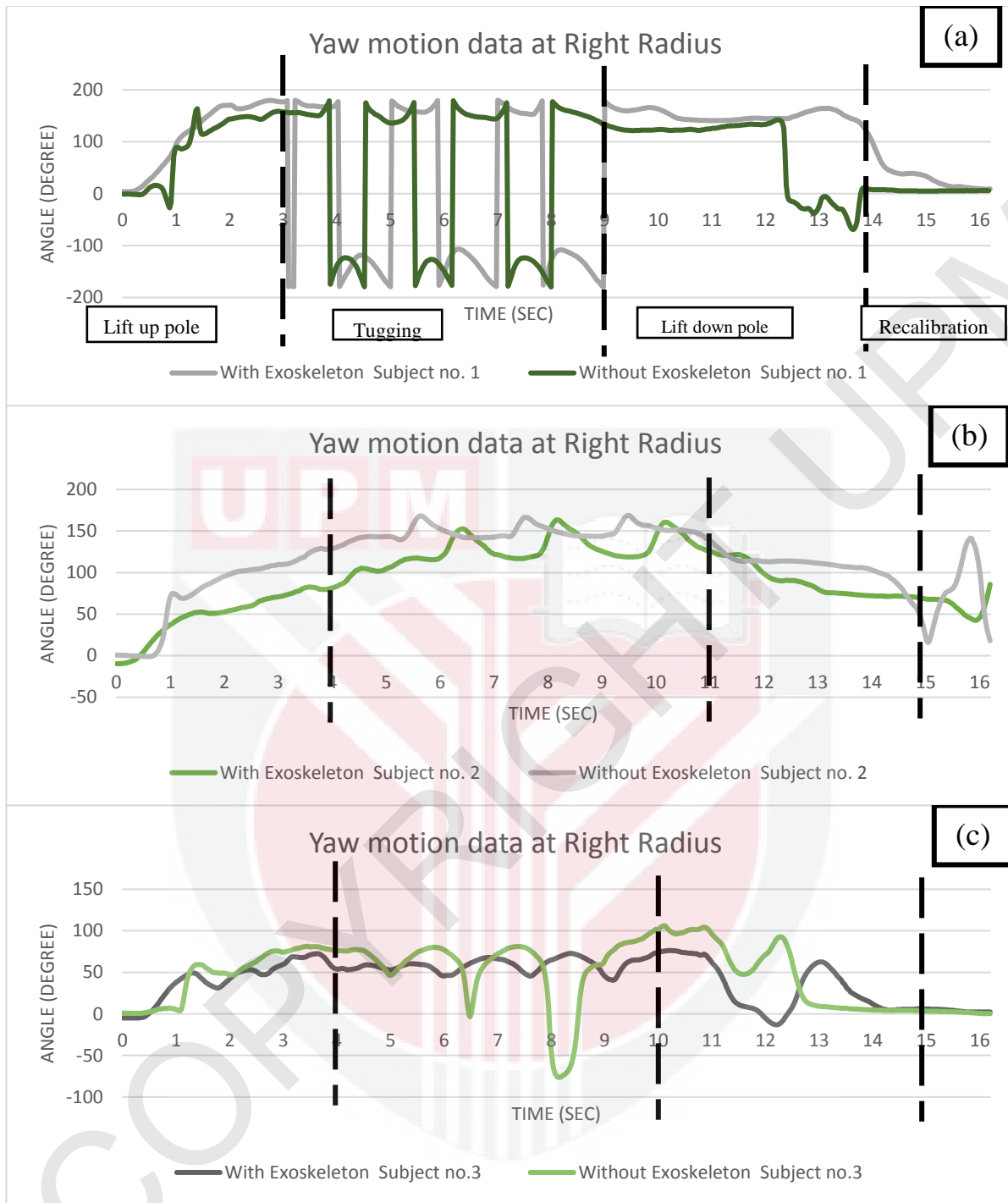


Figure 4.27: Graphs for yaw motion data at right radius. (a) Subject number 1. (b) Subject number 2. (c) Subject number 3.

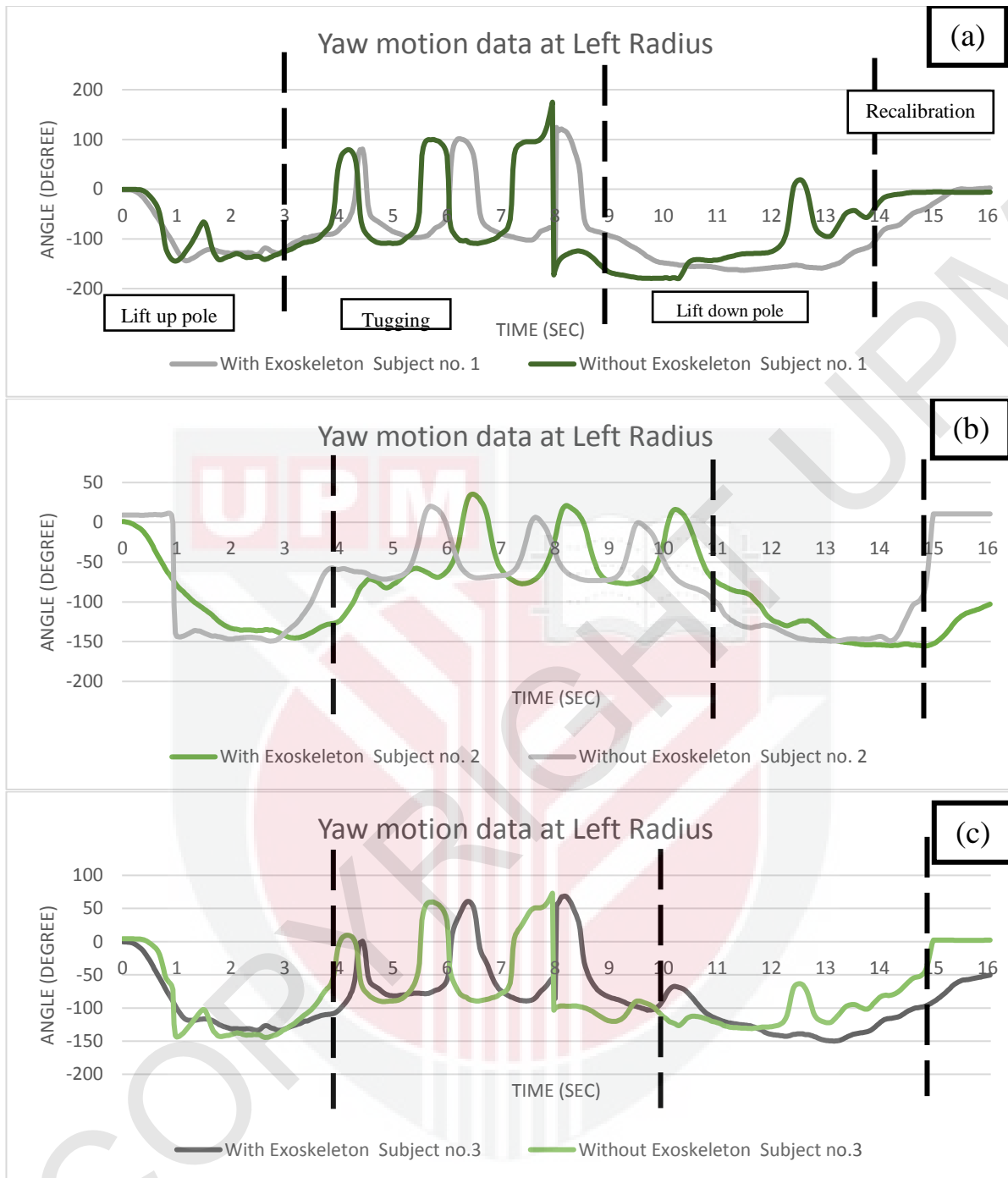


Figure 4.28: Graphs for yaw motion data at left radius. (a) Subject number 1. (b) Subject number 2. (c) Subject number 3.

Figure 4.27 show graphs for yaw motion data at right radius and Figure 4.28 graphs for yaw motion data at left radius. When referred at left radius and right radius yaw motion data (Figure 4.27 and Figure 4.28), we are able to determine left radius and right radius rotation on z-axis. For both left and right radius (Figure 4.27 and Figure 4.28), we able to understand that exoskeleton does not impose the restriction towards the angle of motion. So, the left and right radius abduction and adduction (Figure 4.22) does not affected by exoskeleton.

However, all of the yaw motion graphs when wearing exoskeleton for all subjects at left and right shows one second delay. This shows that by wearing exoskeleton, the subject movements are tend to be delay.

Chapter 5: Conclusion and Recommendation

5.1 Conclusion

Exoskeletons are wearable devices used to assist the workers. Many upper limbs exoskeletons may assist lifting as well as upholds the labourers' arm in activities from chest to overhead. Implementation of the exoskeletons is to prevent excessive muscle straining among the plantation workers.

When designing exoskeleton, we need the subject's movement to be predicted so we able to minimize discomfort. To help understand the impact of exoskeleton on the user, we used IMU sensors to measure the subject's limbs movement. From the experiment, we able to demonstrate that that exoskeleton had few advantages to the subjects.

The advantages is wearing exoskeleton will helps to reduced muscle activity. The reason is because when wearing an exoskeleton, the subject's angle of movement are much lower because the movement is restricted by the exoskeleton.

However, there is also one disadvantage when wearing exoskeleton which is causing time delay. The subject body movement delay may cause by the restriction at some part of exoskeleton such as supports and spring under the arms or when the exoskeleton harness was fasten at the subject's body.

5.2 Recommendation

5.2.1 Recommended workflow

A few significant points have to be kept in mind to generate the most precise information from inertial movement trackers. As explained in the discussion the MTw Awinda orientation estimate is based on a Kalman filter, which usually sequentially processes information and develops with time a brief moment shortly after start-up (10s to 15s) without or with motions, preferably without magnetic distortions. The method is known as "warm up filter."

It is suggested to avoid cuts during recording and to minimize time intervals with wireless disconnections, so that buffer overflow is prevented. Throughout and at the end of recording, information packets stored are transferred. With the MTw's well within the Awinda Master wireless range this method will be more effective.

5.2.2 Future of this project

In the future, we will focus more on the analysis of the exoskeleton based on joint angle rather than only comparing the body limbs' angle of motion. The reason to introduce new parameter when analyse the exoskeleton, is to help us to understand more on how far that an exoskeleton will impact the workers movement. Estimation of joints angle should also give better understanding on how much the exoskeleton will restrict the subjects' limbs movement.

References

- Abdul Razak Jelani, Ahmad Hitam, Johari Jamak, Malik Noor, Yosri Gono, Omar Ariffin, 2008. Cantas™ - A tool for the efficient harvesting of oil palm fresh fruit bunches. *J. Oil Palm Res.* 20, 548–558.
- Ahmad, N., Ghazilla, R.A.R., Khairi, N.M., Kasi, V., 2014. Reviews on Various Inertial Measurement Unit (IMU) Sensor Applications. *Int. J. Signal Process. Syst.* 1, 256–262.
- Akdoğan, E., 2019. Design, Produce and Control of a 2-Dof Upper Limb Exoskeletal Robot. *J. Therm. Eng.* 5, 119–130.
- Cavallo, A., Cirillo, A., Cirillo, P., De Maria, G., Falco, P., Natale, C., Pirozzi, S., 2014. Experimental comparison of sensor fusion algorithms for attitude estimation, *IFAC Proceedings Volumes (IFAC-PapersOnline)*. IFAC.
- Gonzalez, C., 2017. Manufacturing Workers Become More than Human with Exoskeletons | *Machine Design* [WWW Document]. Dec. 07. URL <https://www.machinedesign.com/motion-control/manufacturing-workers-become-more-human-exoskeletons> (accessed 4.24.19).
- Hirose, K., Doki, H., Kondo, A., 2013. Dynamic analysis and motion measurement of ski turns using inertial and force sensors. *Procedia Eng.* 60, 355–360.
- Jain, P., n.d. What is Magnetometer: Types & Applications [WWW Document]. 2012. URL <https://www.engineersgarage.com/articles/magnetometer> (accessed 4.30.19).
- Kajānek, P., n.d. Testing of the Possibilities of Using IMUs with Different Types of Movements 61–66.
- Labs, Y., 2013. Yost - Calculating Angles Between Two Yost Labs 3-Space Sensor™ Devices

on a Human Body 23.

Ma, Y., Ma, Y., 2011. General Principles of Treating Soft Tissue Dysfunction in Sports Injuries. *Acupunct. Sport. Trauma Rehabil.* 212–233.

Matula, T., 2016. Estimating Human Movement Using Accelerometers 33.

Modic, E., 2018. Exoskeletons support BMW line workers in South Carolina - Today's Motor Vehicles [WWW Document]. Today'smotorvehicles. URL <https://www.todaysmotorvehicles.com/article/exoskeletons-support--bmw-line-workers-in-south-carolina/> (accessed 4.24.19).

Namikawa, K., 2012. Agricultural robot. *J. Robot. Soc. Japan* 8, 111–112.

O'Donovan, K.J., Kamnik, R., O'Keeffe, D.T., Lyons, G.M., 2007. An inertial and magnetic sensor based technique for joint angle measurement. *J. Biomech.* 40, 2604–2611.

Paulich, M., Schepers, M., Rudigkeit, N., Bellusci, G., 2018. Xsens MTw : Miniature Wireless Inertial Motion Tracker for Highly Accurate 3D Kinematic Applications. *Xsens Technol.* 1–9.

Pérez, R., Costa, Ú., Torrent, M., Solana, J., Opisso, E., Cáceres, C., Tormos, J.M., Medina, J., Gómez, E.J., 2010. Upper limb portable motion analysis system based on inertial technology for neurorehabilitation purposes. *Sensors* 10, 10733–10751.

Saibani, N., Muhamed, A.A., Maliami, M.F., Ahmad, R., 2015a. Time and Motion Studies of Manual Harvesting Methods for Oil Palm Fruit Bunches: A Malaysian Case Study. *J. Teknol.* 74.

Saibani, N., Muhamed, A.A., Maliami, M.F., Ahmad, R., 2015b. Time and motion studies of manual harvesting methods for oil palm fruit bunches: A Malaysian case study. *J. Teknol.* 74, 77–83.

Seel, T., Raisch, J., Schauer, T., 2014. IMU-based joint angle measurement for gait analysis. *Sensors (Switzerland)* 14, 6891–6909.

Toyama, S., Yamamoto, G., 2009. Development of Wearable-Agri-Robot ~mechanism for agricultural work~. In: 2009 IEEE/RSJ International Conference on Intelligent Robots and Systems. IEEE, pp. 5801–5806.

Yagi, E., Harada, D., Kobayashi, M., 2016. Upper-Limb Power-Assist Control for Agriculture Load Lifting. *Int. J. Autom. Technol.* 3, 716–722.



Appendix

Standard Operating Procedure

Hardware



Figure above: Docking station and dongle known as master for data transmission.

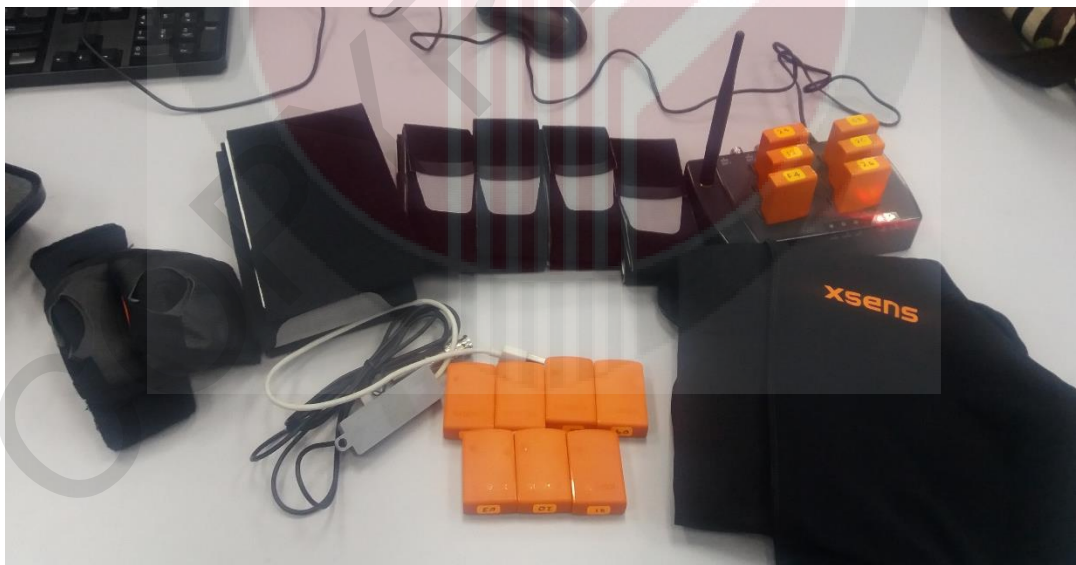
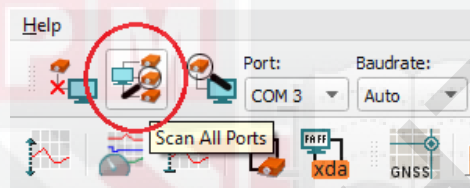


Figure above: From left: head band, glove, Velcro straps, station and IMUs, shirt, IMUs and timer trigger hardware.

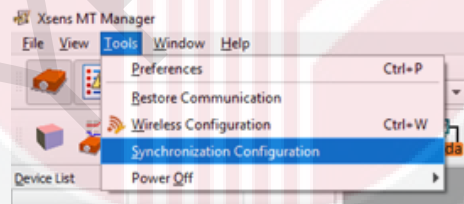
Setting Up Hardware Connection

1. Place all the MTw's into the slots (docking area) on the Awinda station.
2. Connect the Awinda station into the laptop via USB cable or connect the Awinda USB dongle into the laptop (if necessary)
3. Open up the **MT Manager** application from the desktop
4. The software (MT Manager) should automatically scan all ports for hardware connection.

If not, click on the **Scan All Ports** icon from the toolbar menu



5. To add timer trigger, click on Synchronization Configuration, then set the desired trigger setting and save.



6. To start measurement, remove MTw's from the Awinda station, and click on **wireless configuration** to connect wirelessly to the available Master (Awinda station or dongle).

Enable All Wireless Master to detect the MTw's then **Start Measurement on All Wireless Masters**, and close. Below is an example of 3 MTw's that are **wirelessly connected** to the Awinda station (**Wireless Configuration** window activated to show connectivity and signal strength).

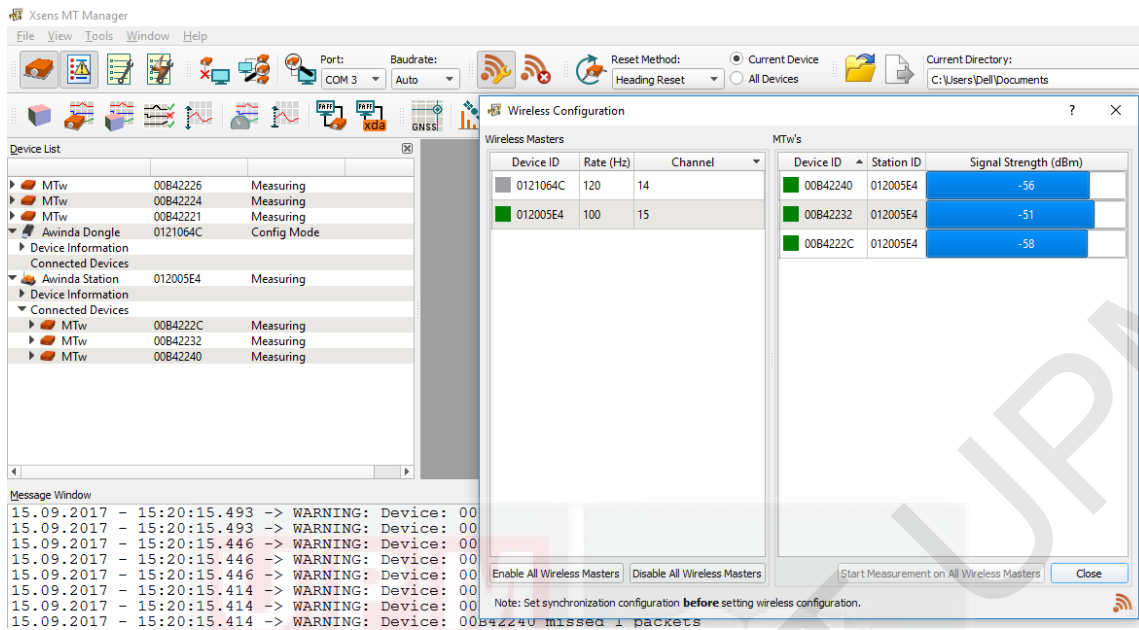


Figure above: xsens MT Manager Interference

Inertia Motion Unit (Mtw) Placement



Figure above: Sensors placement (front view)



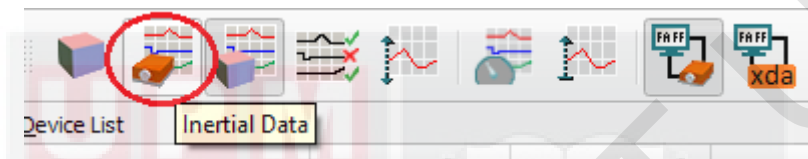
Figure above: Sensors placement (side view)



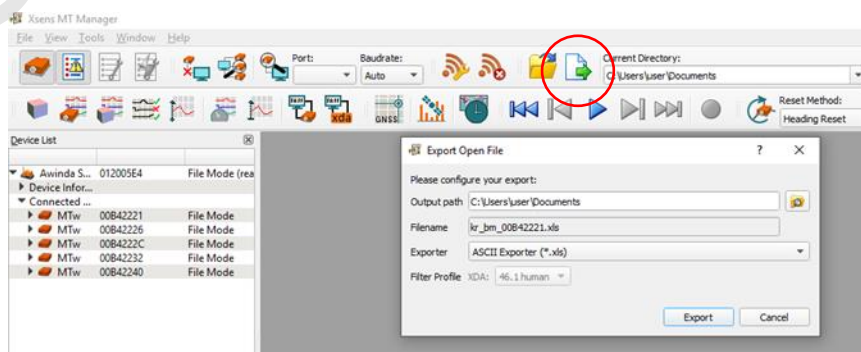
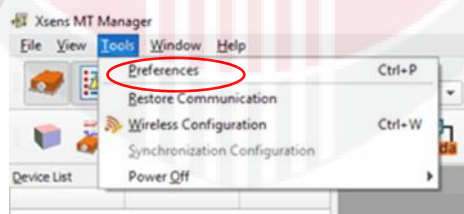
Figure above: Sensors placement (backside view)

Monitoring Mtw

1. With the MTw's wirelessly connected to Awinda Master (whether Awinda station or Awinda USB dongle) their status can be measured and tracked via several tools. For example, clicking on the **Inertial Data** icon will allow users to monitor **Acceleration**, **Angular velocity**, and **Magnetic field** for the corresponding MTw.



2. To record a file, press the **Record** icon (red circle) from the toolbar menu and end the recording once done. Log files can then be retrieved for further scrutiny and analyzed.
3. To export the recorded data, open the saved log files, edit the preference of data that need to be exported. Click on white sheet on toolbars to export the data files. For example inertial data in Excel files.



Additional Information

Wireless update rates	
1 MTw	120 Hz
5 MTw	120 Hz
9 MTw	100 Hz
10 MTw	80 Hz
20 MTw ²	60 Hz

Wireless update rates depends on the number of IMU in use, kindly change the rate before start measuring at the Synchronization Configuration.

Communication			
Range	Awinda station	Awinda dongle	
Open space	Up to 50 m (165 ft.)	Up to 20 m (65 ft.)	
Office space	Up to 20 m (65 ft.)	Up to 10 m (33 ft.)	
Wireless protocol	Xsens patented Awinda protocol ¹		
Receiver	Awinda Station / Awinda Dongle		
Orientation			
Static Accuracy (Roll/Pitch)	0.5 deg RMS		
Static Accuracy (Heading)	1 deg RMS		
Dynamic Accuracy (Roll/Pitch)	0.75 deg RMS		
Dynamic Accuracy (Heading)	1.5 deg RMS		
Tracker components			
	Angular velocity	Acceleration	Magnetic field
Dimensions	3 axes	3 axes	3 axes
Full scale	± 2000 deg/s	± 160 m/s ²	± 1.9 Gauss